

2015

Sequence Stratigraphy and Reservoir Characterization of the Middle Devonian Marcellus Formation for a Cored Well in Harrison County, West Virginia

Victoria L. Hilliard

Follow this and additional works at: <https://researchrepository.wvu.edu/etd>

Recommended Citation

Hilliard, Victoria L., "Sequence Stratigraphy and Reservoir Characterization of the Middle Devonian Marcellus Formation for a Cored Well in Harrison County, West Virginia" (2015). *Graduate Theses, Dissertations, and Problem Reports*. 5805.

<https://researchrepository.wvu.edu/etd/5805>

This Thesis is protected by copyright and/or related rights. It has been brought to you by the The Research Repository @ WVU with permission from the rights-holder(s). You are free to use this Thesis in any way that is permitted by the copyright and related rights legislation that applies to your use. For other uses you must obtain permission from the rights-holder(s) directly, unless additional rights are indicated by a Creative Commons license in the record and/ or on the work itself. This Thesis has been accepted for inclusion in WVU Graduate Theses, Dissertations, and Problem Reports collection by an authorized administrator of The Research Repository @ WVU. For more information, please contact researchrepository@mail.wvu.edu.

**Sequence Stratigraphy and Reservoir Characterization of the Middle Devonian
Marcellus Formation for a Cored Well in Harrison County, West Virginia**

Victoria L. Hilliard

Thesis submitted to the
Eberly College of Arts and Sciences
at West Virginia University
in partial fulfillment of the requirements
for the degree of

Master of Science

In

Geology

Timothy Carr, Ph.D., Chair

Jaime Toro, Ph.D.

Thomas Wilson, Ph.D.

Department of Geology and Geography

Morgantown, West Virginia

2015

Keywords: Marcellus Formation; Sequence Stratigraphy; ECS Lithofacies; Total Organic
Carbon; Transgressive – Regressive Sequences; Brittleness

Copyright 2015 Victoria Hilliard

ABSTRACT

Sequence Stratigraphy and Reservoir Characterization of the Middle Devonian Marcellus Formation for a Cored Well in Harrison County, West Virginia

Victoria L. Hilliard

The Middle Devonian Marcellus Formation is an important unconventional shale play in North America. It has an approximate aerial extent of 100,000 square-miles and has been estimated to contain upwards to 489 trillion cubic feet of recoverable gas. Through the advent of horizontal drilling, in combination with hydraulic fracture stimulation, the Marcellus Formation has been exploited at exponential rates. In order to increase production and drill more profitable wells, the geology of the Marcellus is being studied in more detail. In particular, geologic parameters such as geomechanical properties, total organic carbon (TOC), porosity, and mineralogy could have a direct relationship with the sequence stratigraphy of shale.

To evaluate the geologic parameters that could impact production, core data and well logs taken from the Goff #55 well were compared to one another. A detailed core description of the Marcellus Formation was performed on the core taken from the study well, and used to build a stratigraphic column. The Marcellus Formation was classified into seven lithofacies using advanced mineralogical logs, core X-ray diffraction (XRD), core X-ray fluorescence (XRF), and TOC data. Geomechanical properties were calculated using Poisson's ratio, Young's modulus, and mineralogy. The Marcellus Formation was divided into three intervals based on transgressive-regressive sequences and the associated boundaries by using common and advanced well logs. Lastly, a regional sequence stratigraphy was developed using approximately forty wells surrounding the Goff #55 well.

ACKNOWLEDGEMENTS

I would like to express my sincere gratitude to the Geology Department of West Virginia University for providing funding and support for graduate school. I would like to thank my advisor Dr. Tim Carr for his patience and guidance throughout this research, and for always tolerating unannounced and repeated pop-ins to your office. I would also like to thank my committee members Dr. Jaime Toro and Dr. Thomas Wilson for your helpful suggestions on this research and the invaluable knowledge gained from your courses. Special acknowledgements must be given to Shuvajit Bhattacharya and Chloe Wonnell for sharing your advice, knowledge, and experience. Without realizing it, you both helped revitalize this research every time I visited your office. Also, thank you Shuvajit for providing the ECS Facies for this study. Special thanks goes to John Baird for all your help and friendship over the past two years. Thank you for the time spent talking, bouncing ideas back and forth, patience, and being a great office mate.

Thank you to all my friends for being there for me in so many ways. Most importantly, I would like to give thanks to my family. I would not be the person I am today if it were not for your guidance, sacrifices, support, and unending love. Your encouragement and understanding has given me the courage to reach for my goals and venture forward in life. I would especially like to thank my sisters for being my rock and best friends in life. Finally, I would like to thank God for all of the opportunities and experiences he has made possible.

TABLE OF CONTENTS

INTRODUCTION	1
Purpose	1
Study Area.....	2
Geologic History	3
Depositional Environment and Sequence Stratigraphy	5
METHODS AND RESULTS	8
Well Logs	8
Total Organic Carbon (TOC)	11
Tops	13
ECS Lithofacies.....	15
Geomechanics	18
Physical Core.....	21
Regional Sequence Stratigraphy	29
DISCUSSION	36
TOC & Pyrite	36
Geomechanics	37
ECS Lithofacies.....	39
Marcellus Formation	41
Lower Marcellus.....	43
Middle Marcellus	45
Upper Marcellus.....	46
Regional Sequence Stratigraphy	47
CONCLUSION	48
REFERENCES	51
APPENDIX	55
Core Description.....	55

TABLE OF FIGURES:

Figure 1. The study area in Harrison County, West Virginia.	3
Figure 2. Tectonic reconstruction of Laurentia’s eastern margin during the Middle Devonian (385Ma), showing the Appalachian Basin and various structural features.	4

Figure 3. Diagram illustrating the relationship of lithospheric loading, foreland basin subsidence, and sedimentation into foreland basin.	5
Figure 4. Schematic of the Middle Devonian lithostratigraphy of the Catskill delta in the Appalachian basin.....	7
Figure 5. West to East cross-strike schematic diagram of the Catskill delta.....	8
Figure 6. Cross section for the Goff #55 well.....	10
Figure 7. Cross plot of computed TOC and core measured TOC.....	11
Figure 8. Relationship between core measured XRD values of TOC and bulk density	12
Figure 9. Relationship between estimated TOC and core measured XRD values of pyrite	12
Figure 10: Sequence stratigraphic model of sea level rise and fall.	14
Figure 11: Cross section of the gamma ray log for the Goff #55 study well.....	15
Figure 12: Workflow utilized to classify lithofacies of the Marcellus Formation.....	17
Figure 13. Graph of the abundance of different lithofacies present in the upper, middle, and lower Marcellus Formation.....	17
Figure 14. Cross plot of the ECS lithofacies versus brittleness, and shaded with TOC estimated	18
Figure 15. Cross plot of Poisson's Ratio and Young's Modulus shaded with brittleness computed using the brittleness average method	20
Figure 16. Cross plot of Poisson's Ratio and Young's Modulus shaded using brittleness computed by using the brittleness index method.....	21
Figure 17. The stratigraphic column made from core descriptions	26
Figure 18. The scaled stratigraphic column and well logs are plotted next to one another	29
Figure 19. Map of West Virginia showing wells with gamma ray, bulk density, neutron porosity, or density porosity logs, and cross-section lines.....	30
Figure 20. Along strike cross section (A- A') flattened on the top of the Tully Formation.....	31
Figure 21. Down dip cross section (B- B') flattened on the top of the Lower (L.) Marcellus.....	32
Figure 22. Down dip cross section (B- B') flattened on the top of the Middle (M.) Marcellus...	32
Figure 23. Down dip cross section (B- B') flattened on the top of the Upper (U.) Marcellus.....	33
Figure 24. Down dip cross section (B- B') flattened on the top of the Mahantango.....	34
Figure 25. Down dip cross section (B- B') flattened on the top of the Tully.....	35
Figure 26: Cross-section of the Goff #55 study well.....	37
Figure 27. Cross plot of Poisson's Ratio and Young's Modulus shaded by ECS Lithofacies.....	39
Figure 28: 2D SEM image taken of the core at 7,122ft.....	42

Figure 29: 2D SEM image taken of the core at 7,128ft.....	43
Figure 30. Photo taken of the core showing pockets of ash.....	45

TABLE OF EQUATIONS:

Equation 1. Schmoker's (1993) equation to estimate TOC (Vol. %)	11
Equation 2. Poisson's Ratio (ν) equation.....	19
Equation 3. Young's modulus (E) equation	19
Equation 4. Equation to normalize Poisson's Ratio	19
Equation 5. Equation to normalize Young's Modulus	19
Equation 6. Brittleness index (BI) equation	20

INTRODUCTION:

Of all the gas plays in the United States, the Marcellus Formation is the largest. It covers approximately 100,000 square-miles, six states, and has been estimated to contain 50 to 489 trillion cubic feet (Tcf) of recoverable gas (NETL 2010, 2013). In 2004, Range Resources Corporation drilled the first economically successful vertical well targeting the Marcellus Formation by using similar hydraulic fracture stimulation techniques employed in Texas for the Barnett Shale, and in 2007, completed the first significant horizontal well (Zagorski et al., 2012). Since that time exploitation of the play has increased exponentially, and has had a profound impact on the economy.

During its infancy of exploration, shale plays were considered to be and treated as a homogenous rock with little variation in rock properties. However, after the drilling of many wells, with varying degrees of success and failure, the new school of thought is that shale reservoirs are more complex than originally considered. Geologic parameters such as geomechanical properties, total organic carbon (TOC), porosity, and mineralogy have a direct relationship with the sequence stratigraphy of shale that was not originally recognized in the initial phases of exploration. The sequence stratigraphy and associated geologic parameters of the shale has a significant but poorly understood impact on the recovery potential and production of the natural gas. The proposed research focuses on the stratigraphy and geologic parameters of the Marcellus Formation.

Purpose:

The purpose of this thesis research was to evaluate the different shale parameters that may have had an overall impact on the production of a well targeting the Marcellus Formation, and develop a regional sequence stratigraphy. The well under investigation was Goff #55 (API= 47-033-05106) located in Harrison County, West Virginia. During the initial year of production, the Goff #55 well produced 68,627 million cubic feet (mcf) of dry gas (wvges.com).

Often times a well's core, laboratory data, and well logs are not integrated for further comparison and related to possible stratigraphic controls. Depositional setting and sequence

stratigraphy of the Marcellus was determined through the use of core, whole core high definition CT scanning, X-ray fluorescence (XRF) data, and high resolution 2D scanning electron microscope (SEM) imaging. The geomechanical parameters that were evaluated were Poisson's ratio and Young's modulus. The core and lab data was tied back to the well logs, and the correlation between the different geological parameters and the logs were examined. Lastly, by using other wells in the area a regional sequence stratigraphy of the Marcellus Formation was developed.

Study Area:

The study area is located in Harrison County, West Virginia (Fig.1). Harrison County is located within the Allegheny plateau region of the Appalachian basin in northern-central West Virginia. Structurally, Harrison County is bisected by the slightly northeast to south-west trending Wolf Summit anticline (WSA); Goff #55, the study well, is positioned along the hinge of the anticline.

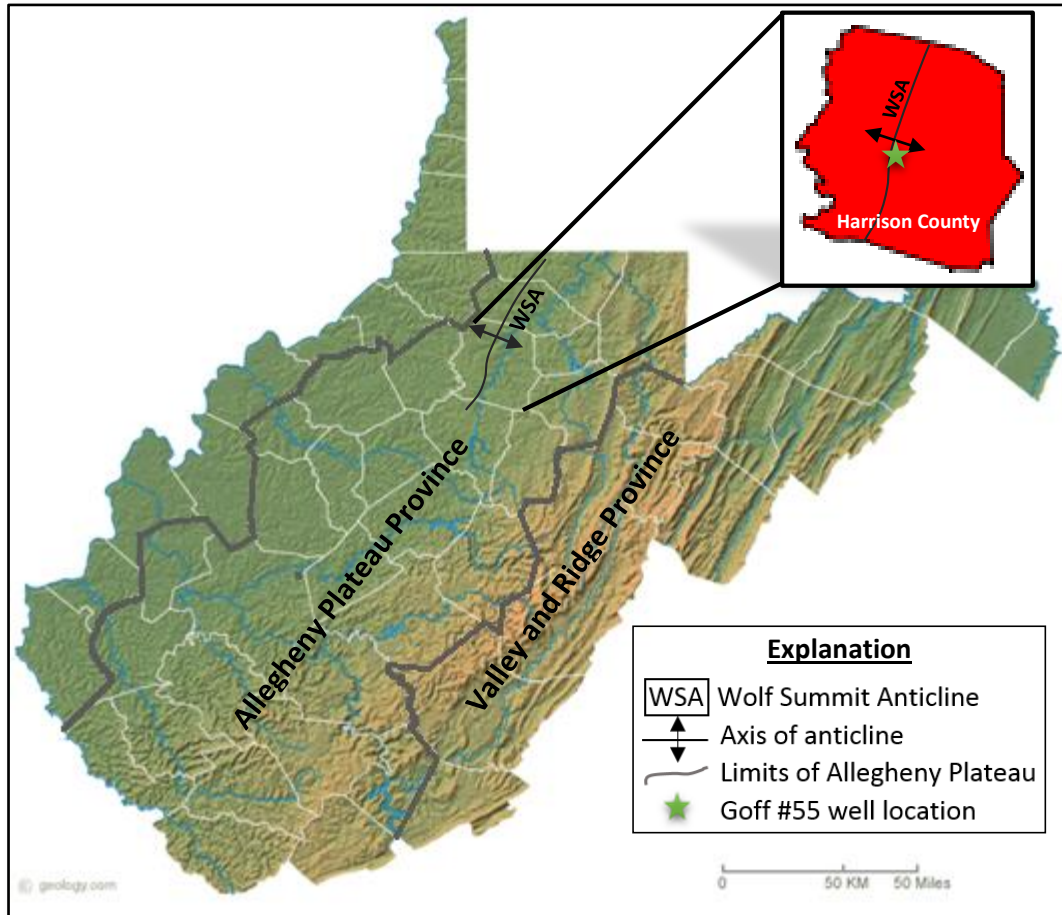


Figure 1. The study area in Harrison County, West Virginia is located in the Allegheny plateau along the Wolf Summit anticline (Modified from geology.com).

BACKGROUND:

Geologic History:

The Devonian Marcellus Formation, part of the Hamilton Group, was deposited in the Catskill delta within the Appalachian basin. The Appalachian basin is an elongate continental basin that formed on the craton side of the Appalachian orogen (Faill, 1997). The Appalachian orogeny extends approximately 3,000 kilometers from Newfoundland to Alabama (Faill 1997, 1985). The Appalachian basin extends westward to the Cincinnati arch, Findlay arch and Algonquin axis (Figure 2) (Faill, 1997).

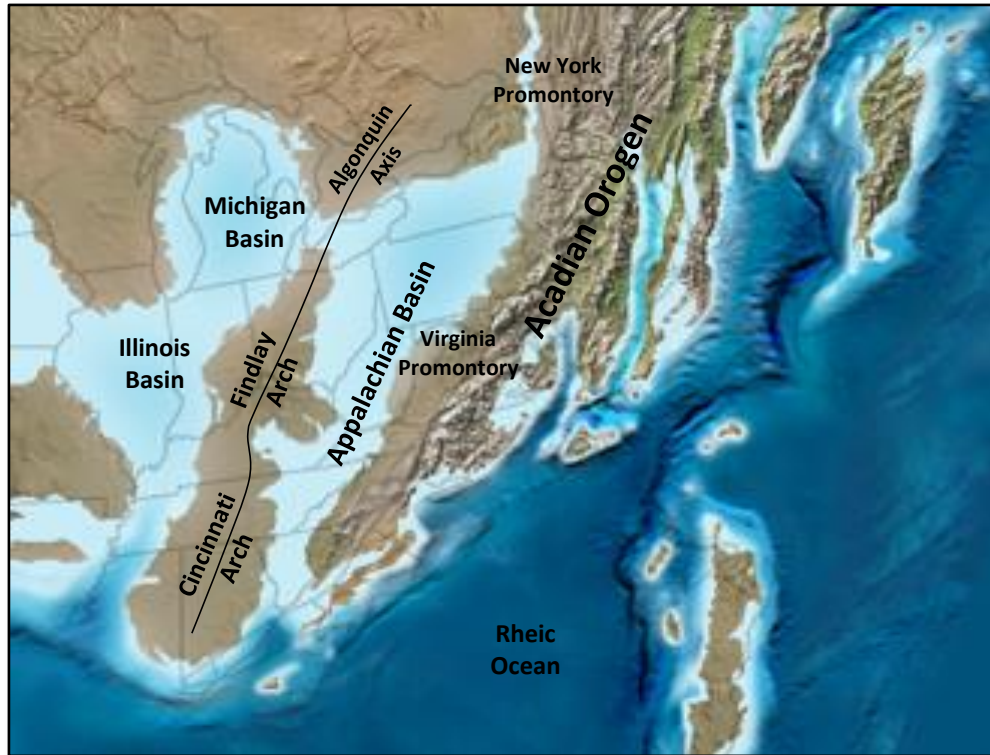


Figure 2. Tectonic reconstruction of Laurentia's eastern margin during the Middle Devonian (385Ma), showing the Appalachian Basin and various structural features. (Modified from Blakey, 2010)

The Appalachian basin was a foreland basin that formed as a result of flexural subsidence induced by lithospheric loading during the Taconic, Acadian, and Alleghanian orogenies (Mabesoone and Neumann, 2005). The Cincinnati, Findlay, and Algonquin arches are interpreted to be the foreland peripheral bulge caused by the lithospheric loading (Figure 3) (Castle, 2001). These arches separated the Appalachian basin from the Illinois and Michigan basins (Faill, 1997). The peripheral bulge and foreland basin migrated westward through time with continued lithospheric loading and crustal shortening (Ettensohn and Brett, 2002).

The Marcellus Formation was deposited as the basal unit of the Catskill delta during the Acadian orogeny. The Acadian orogeny is thought to have begun during the Late Silurian to Early Devonian (421-400 Ma) and to have lasted until the end of the Devonian to Early Carboniferous (395-350Ma) (Staal, 2009). The prevailing theory is that the orogeny occurred due to the oblique convergence and subsequent south westward transcurrent movement of the Avalon terrane along a strike-slip fault (Ettensohn, 1985a). However, there is some evidence that suggest

the segmented deformation was a result of flat-slab subduction, similar to that of the modern Andes (Murphy and Keppie, 2005).

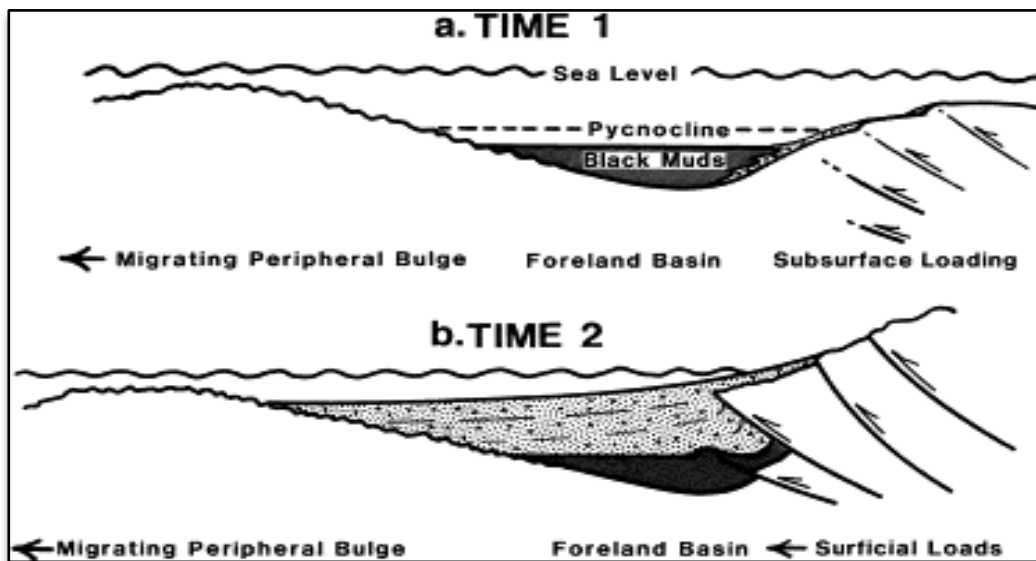


Figure 3. Diagram illustrating the relationship of lithospheric loading, foreland basin subsidence, and sedimentation into foreland basin. (a) Time 1: Beginning of orogenic activity, subsidence of the foreland basin, and deposition of black shales. (b) Time 2: Continued flexural relaxation and basin subsidence with deposition of coarser sediments. (Ettensohn and Brett, 2002)

Depositional Environment and Sequence Stratigraphy:

The Devonian aged Marcellus Formation is an organic rich, black shale that directly overlies the fossiliferous, argillaceous limestone of the Devonian Onondaga Limestone (Fig. 4). The Marcellus Formation is the basal unit of the Hamilton Group, which were the first deposits of the Catskill delta in the Appalachian basin (Fig. 5) (Ettensohn, 1985a). The upper portion of the Hamilton Group is composed of the Mahantango Formation, which is a non-organic, gray shale.

The transition from the Onondaga Limestone to the Marcellus Formation is rather abrupt across the basin. This indicates that there was a rapid change in environments from shallow oxygenated waters to deeper suboxic to anoxic bottom waters (Castle, 2011; Lash and Blood, 2014). This dynamic change in lithology is attributed to rapid basin subsidence induced by lithospheric loading and eustatic sea level rise (Ettensohn, 1985a; Brett et al., 2011).

The Catskill delta is Middle- to Late Devonian in age, stretches approximately 800km from the New York to Virginia promontory, ranges in thickness from 2,400m to 3,000m, and is composed of five sequences of marine and non-marine facies (Ettensohn, 1985a, 2004; Woodrow, 1985). The first facies sequence of the Catskill delta is comprised of the Hamilton Group (Fig. 5) (Ettensohn, 1985a). The paleo-environments and associated processes of the Catskill delta ranged from subaerial to aqueous and included alluvial fans, alluvial plains, shoreline, basin margin, and deep basin (Woodrow, 1985). The displacement of the different environments and associated facies was not only a result of transgression and regression, but also a result of the interplay between the effects subsidence and accommodation space (Woodrow, 1985; Ettensohn, 1995a; Brett et al., 2011).

In a study by Lash and Engelder (2011) the Marcellus Formation was divided into two members based on transgressive- regressive sequences. The lower member is the Union Springs Member which is divided from the upper Oatka Creek Member by the Purcell Limestone Member (Fig. 4) (Lash and Engelder, 2011). The Union Springs Member has a higher amount of organic matter than the overlying Oatka Creek Member (Lash and Engelder, 2011). In both members there is a higher concentration of organic matter associated with the transgressive system tracts (TST) than in the regressive system tracts (RST) (Lash and Blood, 2014).

Based on the uranium, molybdenum, Fe/Al, and Th/U concentrations and abundant pyrite framboids it is believed that there was a reducing benthic environment present that facilitated the preservation of organic matter (Lash and Blood, 2014; Castle, 2011). Anoxic bottom water conditions may have been a result of high surface water productivity that rained organic matter down to the ocean floor and caused oxygen consumption to occur at a rate that far exceeded ocean water mixing (Lash and Blood, 2014). These productive surface waters would have spread across the area during periods of transgression and broken down to some degree during periods of regression, thus leading to the higher concentrations of organic matter in TST's (Lash and Blood, 2014). The influx of clastic sediment deeper into the basin during periods of regression could have also facilitated the degradation of organic matter preservation seen in RST's.

Based on paleomagnetic data, during the Middle Devonian the Appalachian basin was at a latitude of within 20 degrees of the equator (Kent, 1985). It would have been a warm, wet subtropical environment with high evaporation rates, and affected by the easterly trade-wind belt

(Kent 1985; Ettensohn 1992). This subtropical environment would have promoted erosion and sedimentation into the basin, stratification of the water column, and high surface water productivity (Kent, 1985).

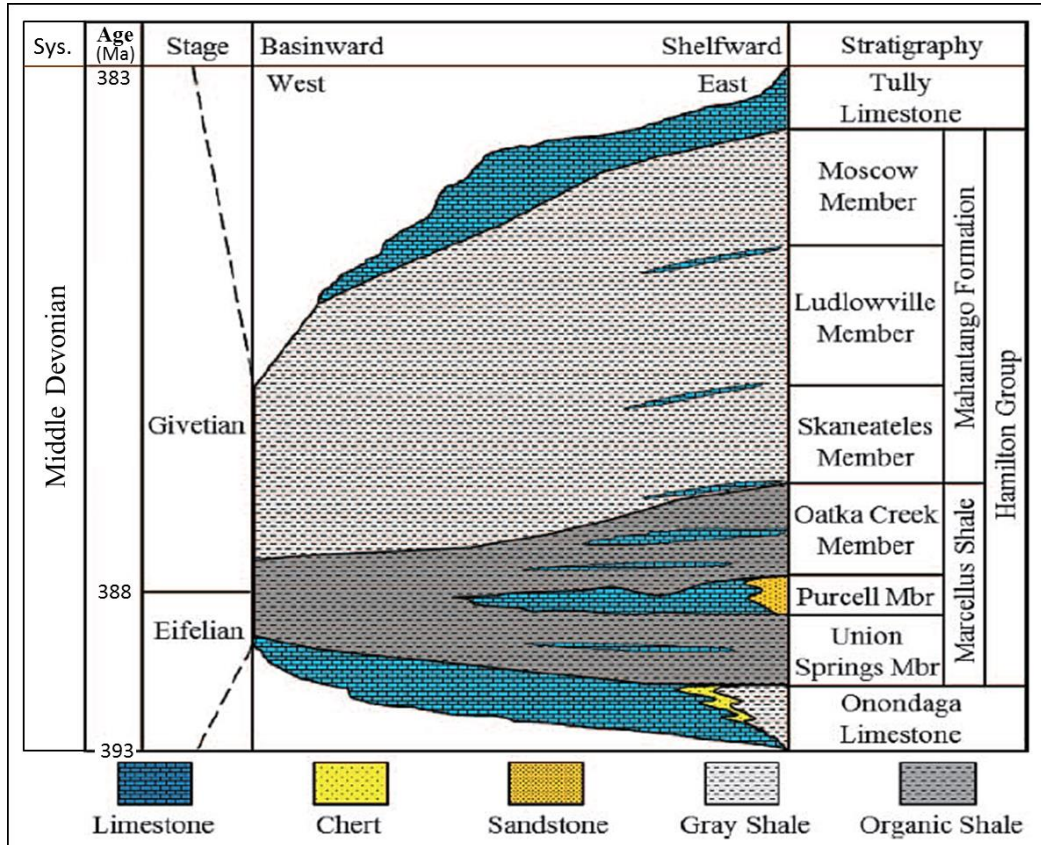


Figure 4. Schematic of the Middle Devonian lithostratigraphy of the Catskill delta in the Appalachian basin from west (basin ward) to east (shelf ward). The Marcellus Formation (labeled Marcellus Shale) and Mahantango Formation have been further subdivided into members. Sys = System (Wang and Carr, 2013).

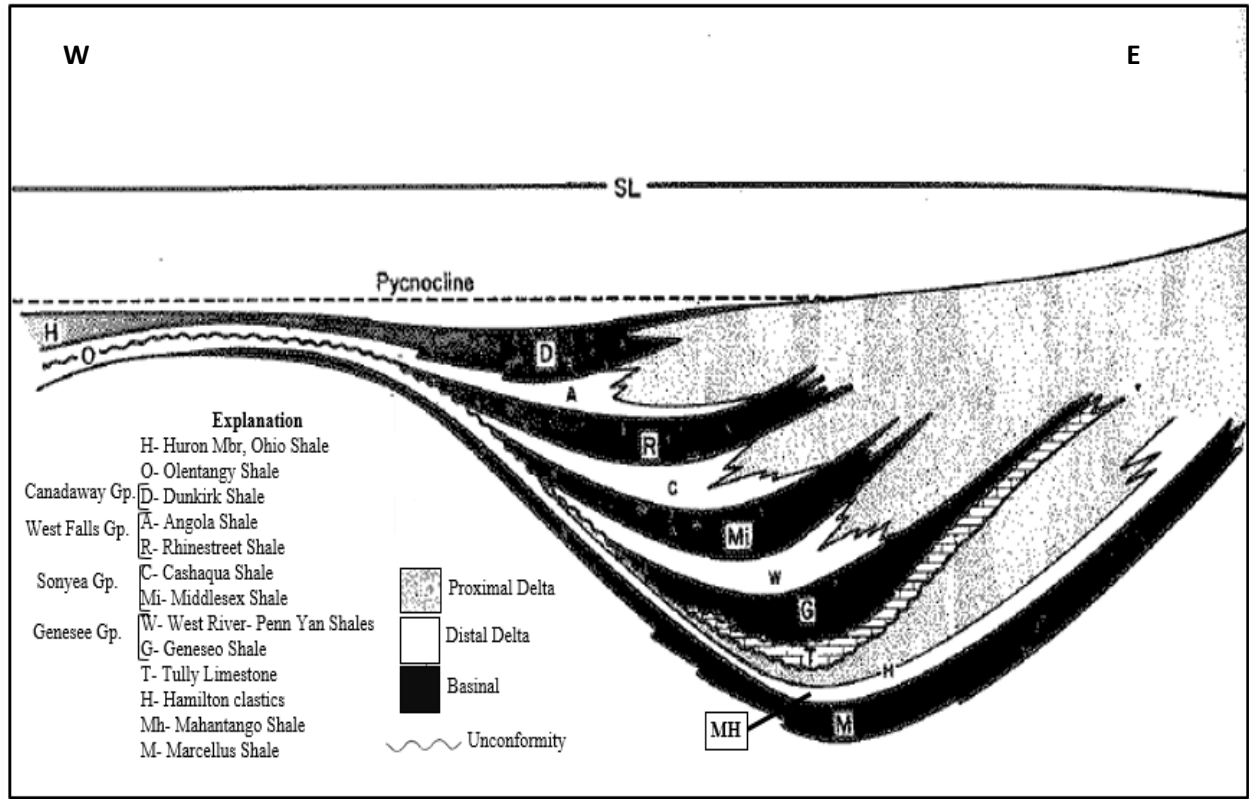


Figure 5. West to East cross-strike schematic diagram of the Catskill delta showing the five facies sequences and the paralic relationship between the proximal delta, distal delta, and basinal environments. Predominately the proximal delta is composed of clastic sediments, the basinal delta contains sandy to silty shales with a low organic content, and the basinal environments have associated organic rich, black shales. Through time, the sequences were displaced westward and the delta prograded cratonward. (Modified from Ettensohn, 1985a).

METHODS AND RESULTS:

Well Logs:

Petroleum Development Corporation provided conventional and advanced well logs for the study well. The suites of logs were uploaded into Petra[®] to aid in the evaluation of the Marcellus Formation. Conventional well logs included gamma ray, caliper, neutron and density porosity, resistivity, bulk density, photoelectric factor, etc. The advanced logs included ELAN[®] mineralogy as a weight percent and volume percent, Spectrolith[®] mineralogy, dipole sonic, hole azimuth, east and north departure, etc.

Once uploaded into Petra[®], the logs were depth shifted so that they would directly match up to the physical core. The logs were also corrected for the east and north departures of the well bore. They were then displayed in cross section view (Fig. 6).

Gamma ray was shaded using “Geo-column” shading so that “hot” zones could easily be seen. These hot, high gamma ray zones correspond to a TOC rich lithology. Caliper was plotted and shaded blue if the reading dropped below 7.875 inches. This was done to indicate if drilling mud was caked along the well bore wall. If the caliper reading was much greater than 7.875 inches then the well bore could have washed out and compromised the integrity other logging tool’s measurements. Very little mud caking or washouts were present in the Marcellus Formation in the study well. Bulk density was shaded blue if it dropped below 2.65 g/cc to indicate probable zones with TOC.

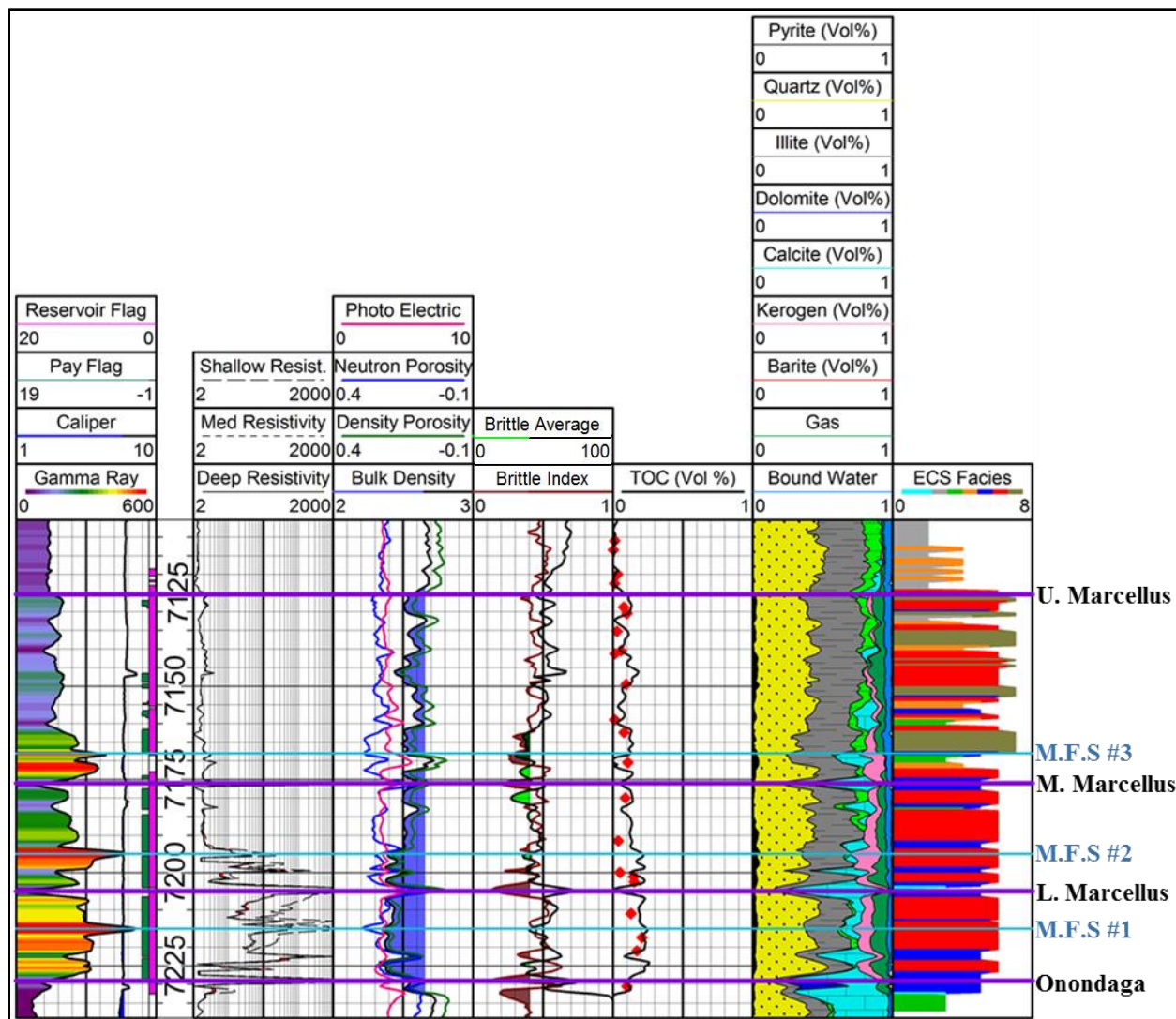


Figure 6. Cross-section for the Goff #55 well. In Track 1 gamma ray is plotted (0 -600 API) and shaded using Geo-column shading, caliper is plotted (1 -10 in) and shaded for values less than 7.875 inches, reservoir and pay flags are also plotted. In Track 2 shallow, medium, and deep resistivity are plotted (2 -2000 ohm-m) on a logarithmic scale. In Track 3 photoelectric factor is plotted (0 -10), neutron and density porosities are plotted (0.4- -0.1), and bulk density is plotted (2 -3 g/cc) and shaded blue for values less than 2.65 g/cc. The brittleness average and brittleness index is plotted in Track 4, and shaded to show when brittleness is less than 40 (the less brittle to ductile zone). In Track 5 total organic carbon (TOC) was estimated using Schmoker's (1979) equation, and is plotted as a volume percent (0-100%). Measured TOC from pyrolysis, and 2D SEM analysis is plotted as red diamonds. In Track 6 ELAN mineralogy is plotted as a volume percent (0-100%). The predicted lithofacies plotted in Track 7 were computed using ELAN mineralogy, estimated TOC, and the classification scheme proposed by Wang (2012). The tops for the Marcellus and Onondaga Limestones are plotted in purple, and maximum flooding surfaces (M.F.S) in blue.

Total Organic Carbon (TOC):

TOC was computed for the study well by Schmoker's (1979) model, which uses formation density logs to estimate TOC as a volume percent (Eq. 1). The model accommodates for calibration bias by using the density from the densest interval of a non-organic, gray shale zone in each individual well. For the study well, there is an 80.7% correlation between the computed and the laboratory measured organic-carbon content (Fig. 7). The estimated TOC was then compared to bulk density (Fig. 8) and pyrite abundance measured from core by x-ray diffraction (XRD) (Fig. 9).

$$TOC (Vol. \%) = \frac{\rho_B - \rho}{1.378} = \frac{2.69 - \rho}{1.378}$$

Equation 1. Schmoker's (1979) equation to estimate TOC as a volume percent (Vol. %), where ρ_B is the density of the densest interval of non-organic, gray shale, and ρ is the bulk density log.

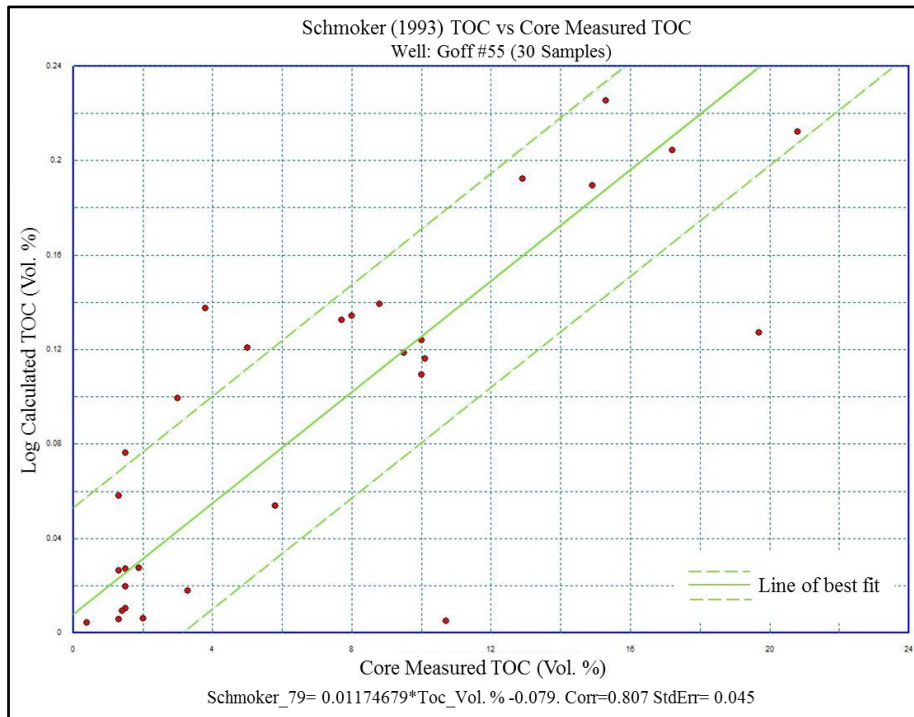


Figure 7. Cross plot of computed TOC using Schmoker's (1979) model and core measured TOC. The data has a correlation of 80.7% and standard error of 0.045.

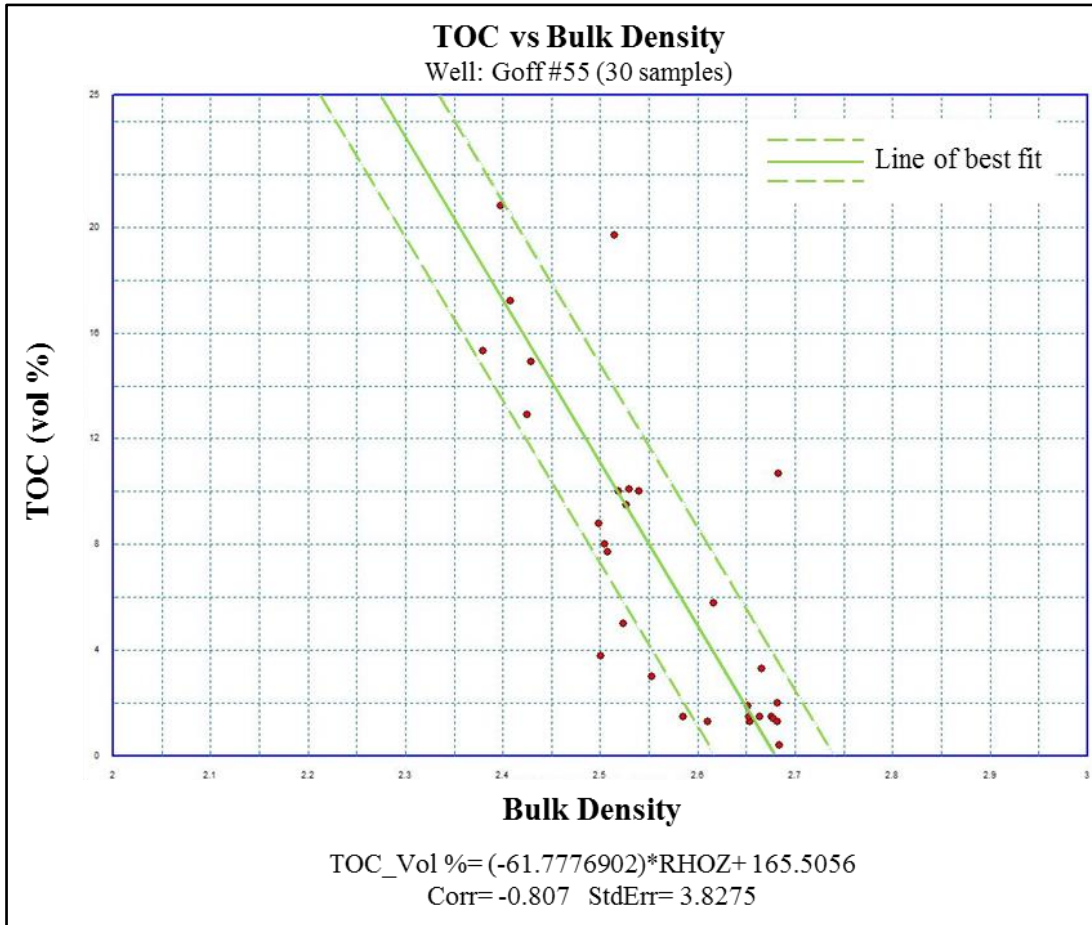


Figure 8. Relationship between core measured XRD values of TOC and bulk density measured by well log.

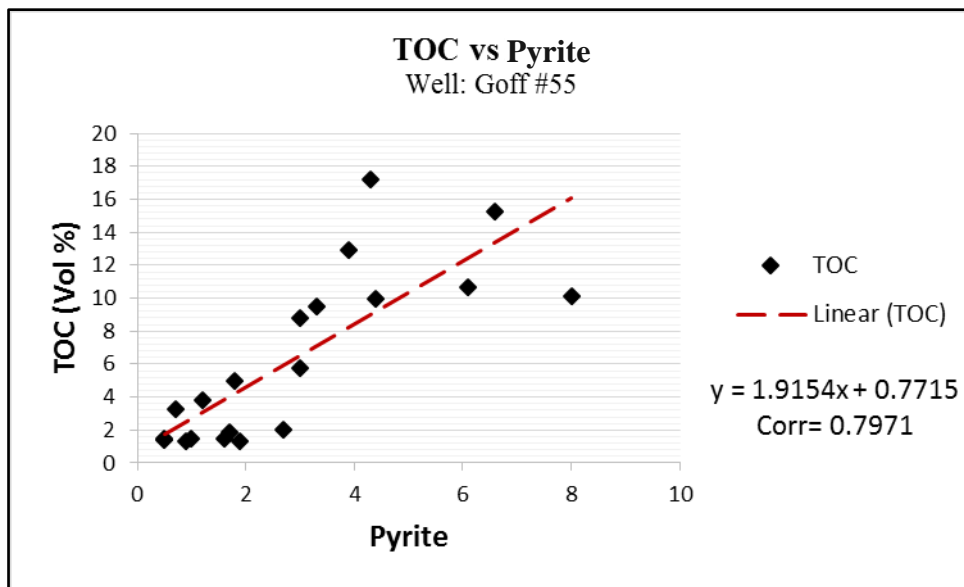


Figure 9. Relationship between estimated TOC and core measured XRD values of pyrite in volume percent.

Tops:

The tops for the formations were chosen primarily based on well logs and crossed checked with the physical core. The tops were not picked solely based on gamma ray because of its coarse resolution. The Onondaga and Marcellus formations top picks may vary up to a few feet from those chosen by the West Virginia Geological Survey and others. Furthermore, the Marcellus Formation was divided into three zones based on the limestone units that defined the cyclic completion of transgressive and regressive system tracts.

The contact between the Onondaga Limestone and Marcellus Formation was gradational over an interval of approximately 4ft (7,232ft -7,228ft) (Fig. 17). The gradational contact consisted of interlayered limestone and shale. The limestone intervals die out from a few inches thick, and the shale layers gradually grow from a few centimeters thick to pure shale. The top for the Onondaga Limestone was picked in the center of the gradation at 7,230ft. This point corresponded to a large spike in the resistivity, which has the finest resolution of all the well logs, and a large jump in gamma ray. Based on the ELAN[®] mineralogical logs, this point is directly above a dolomite-rich layer (Fig. 6)

The Marcellus Formation top was picked at 7,125ft based on where TOC dropped to 0% and bulk density increased to 2.65g/cc. This point also marked where resistivity dropped and remained very low. At this depth, gamma ray dropped and remained below 180API (Fig. 6). This point and characteristic changes in well logs represented a change from a shale with high TOC to a nonorganic shale. In core, the lithology changed from a black shale to a pyrite rich gray shale.

The Marcellus Formation was 105ft (32m) thick in the study well, and was divided into three zones based on major transgressive system tracts (TST) and regressive system tracts (RST). As sea level rises and falls there is an associated change in lithology and grain size deposition that occurs (Fig. 10). As sea level falls the shoreline regresses seaward, and shallower water lithologies and coarser grain sizes are deposited. This characteristic coarsening upward of lithology in a stratigraphic column is referred to as a RST. As sea level begins to rise the shoreline transgresses inland, and finer grain lithologies are deposited. This characteristic fining upward of lithologies in a stratigraphic column is referred to as a TST. If a location was at a depth less than or at wave base then the transition from regression to transgression will be

preserved in the lithologic record as an erosional contact. The erosional surface is the transgressive surface of erosion (TSE). However, if the location was at a depth greater than wave base and no erosion occurred then the point is a correlative conformity (Catuneanu et al., 2009). There was no erosional contact seen in the study well, and the change from an RST to TST was marked by a correlative conformity.

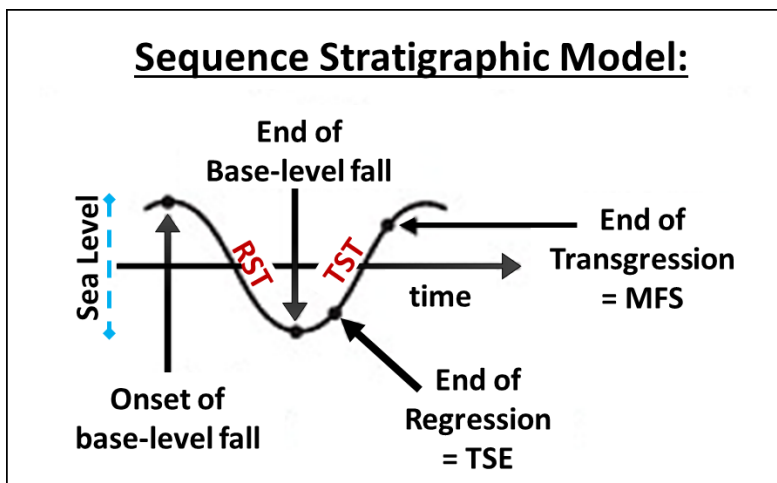


Figure 10: Sequence stratigraphic model of sea level rise and fall. RST= Regressive system tract; TST= Transgressive system tract; MFS= Maximum flooding surface. (Modified from Catuneanu et al., 2009)

The gamma ray log was used to divide the Marcellus Formation into three main units based on completions of transgressive- regressive (T-R) sequences (Fig. 11). The picks were then crossed checked with finer resolution logs and core. If needed the pick would be moved slightly up or down for better placement.

A TST was present at the base of the formation as the lithology changed from a very fossiliferous, shallow water deposited limestone (Onondaga Limestone) into a very fine grained, organic, black silty shale with an increasing gamma ray signature. The first highest peak of the gamma ray was marked as the maximum flooding surface (M.F.S) #1. The gamma ray log immediately dropped after the peak. The drop in gamma ray was associated with a coarsening of lithology, and the lowest point, which is carbonate rich, was chosen to mark the correlative conformity (Fig. 6). The correlative conformity is the top for the lower (L.) Marcellus.

The same method of picking T-R sequences was used to pick tops for the M.F.S #2, middle (M.) Marcellus, and M.F.S #3. The Marcellus Formation top remained the same,

however, it was renamed the upper (U.) Marcellus. The RST associated with the T-R sequence of the U. Marcellus interval does not stop at the U. Marcellus top. It continues until further up the stratigraphic record into the overlying Mahantango Formation.

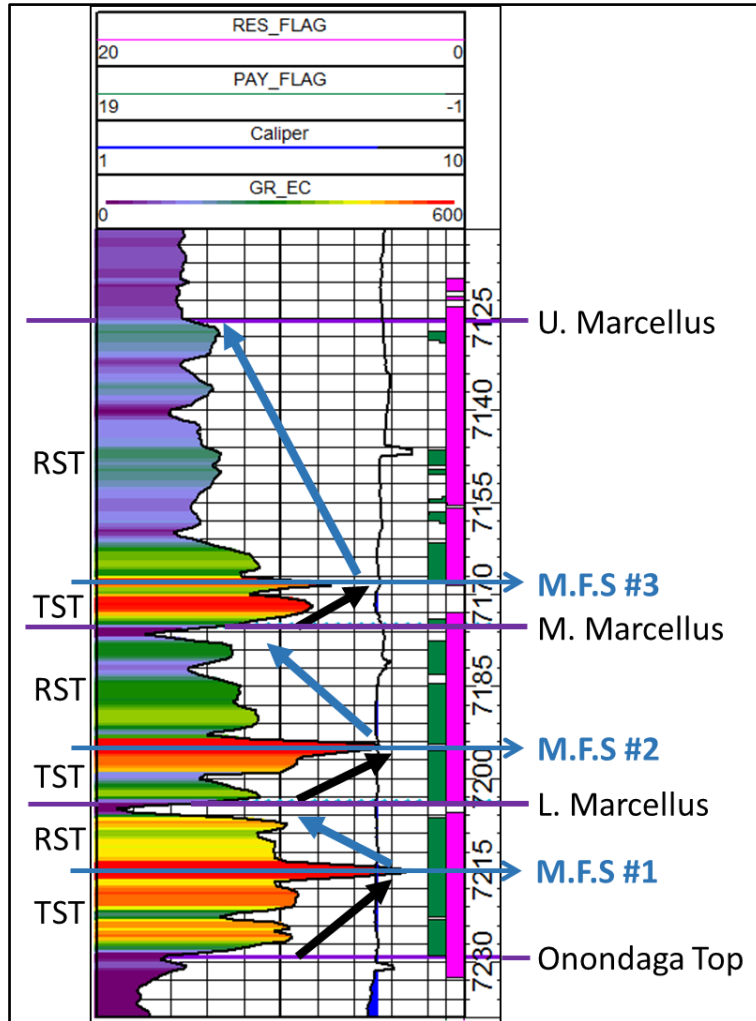


Figure 11: Cross section of the gamma ray log for the Goff #55 study well. The gamma ray log was used to divide the Marcellus Formation into three units based on transgressive-regressive sequences.

ECS Lithofacies:

Shale lithofacies were computed using the techniques and procedures defined by Wang (2012), and utilized advanced ELAN mineralogical logs and core data. There are seven predicted lithofacies present: gray mudstone, carbonate interval, gray mixed shale, gray siliceous shale,

organic mixed shale, organic siliceous shale, and organic mudstone. Lithofacies were classified based on the volume percent of TOC, clay, and the ratio of quartz to carbonate (Fig. 12).

The lithology was said to be organic rich if it had more than 6.0% TOC by volume, this was modified from Wang's (2012) original 6.5% TOC cutoff value. A cutoff value of 40% was used to denote clay-rich lithofacies. This cutoff was chosen because when clay is present in abundance of greater than 40% by volume elastic deformation is dominant (Wang, 2012). Clay volume was computed by summing the amount of illite, chlorite, and kaolinite present.

Lastly, the ratio of quartz to carbonate (RQC) was used to distinguish between carbonate intervals, mixed shale, and siliceous shale. The quartz volume is the summation of quartz, plagioclase, and feldspar. Carbonate volume is the total amount of carbonate and dolomite. If the RQC was less than 1:3 (< 33.3% quartz) the unit was classified as a carbonate interval, if the RQC was greater than 3:1 (> 33.3% carbonate) the lithology was classified as a siliceous shale, and if the RQC was between 1:3 and 3:1 the unit was classified as a mixed shale (Wang, 2012). There was no organic rich carbonate present in the study well.

The ECS lithofacies were plotted next to well logs (Fig. 6) and the stratigraphic column for comparison (Fig. 18). The amount of each lithofacies present in the upper, middle, and lower Marcellus were graphed (Fig. 13). The ECS lithofacies and brittleness index were plotted against each other and shaded by TOC to determine if there was a relationship between the three properties (Fig. 14).

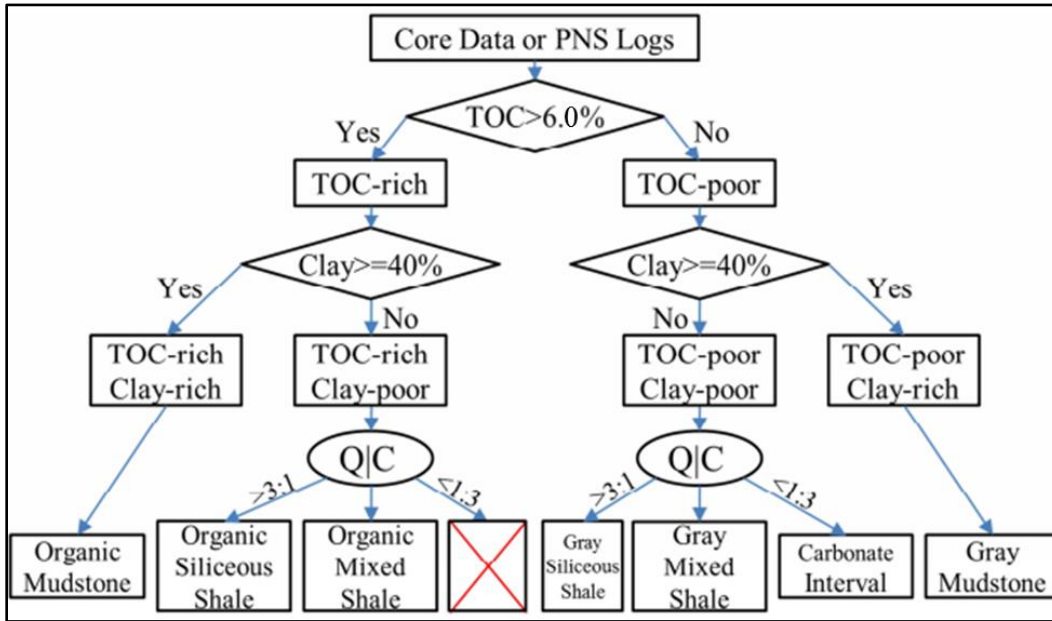


Figure 12: Workflow utilized to classify lithofacies of the Marcellus Formation. (Modified from Wang, 2012)

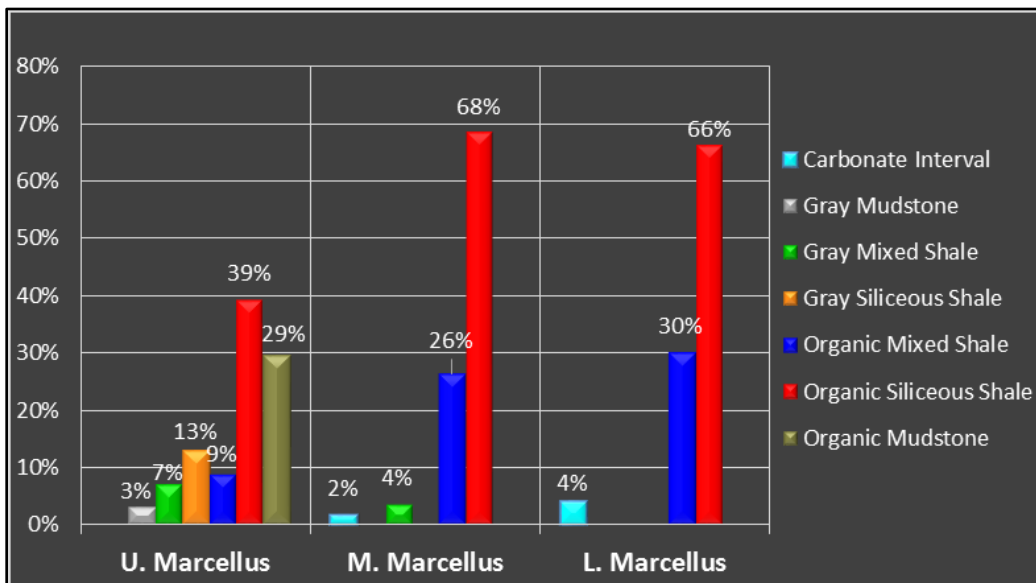


Figure 13. Graph of the abundance of different lithofacies present in the upper, middle, and lower Marcellus Formation.

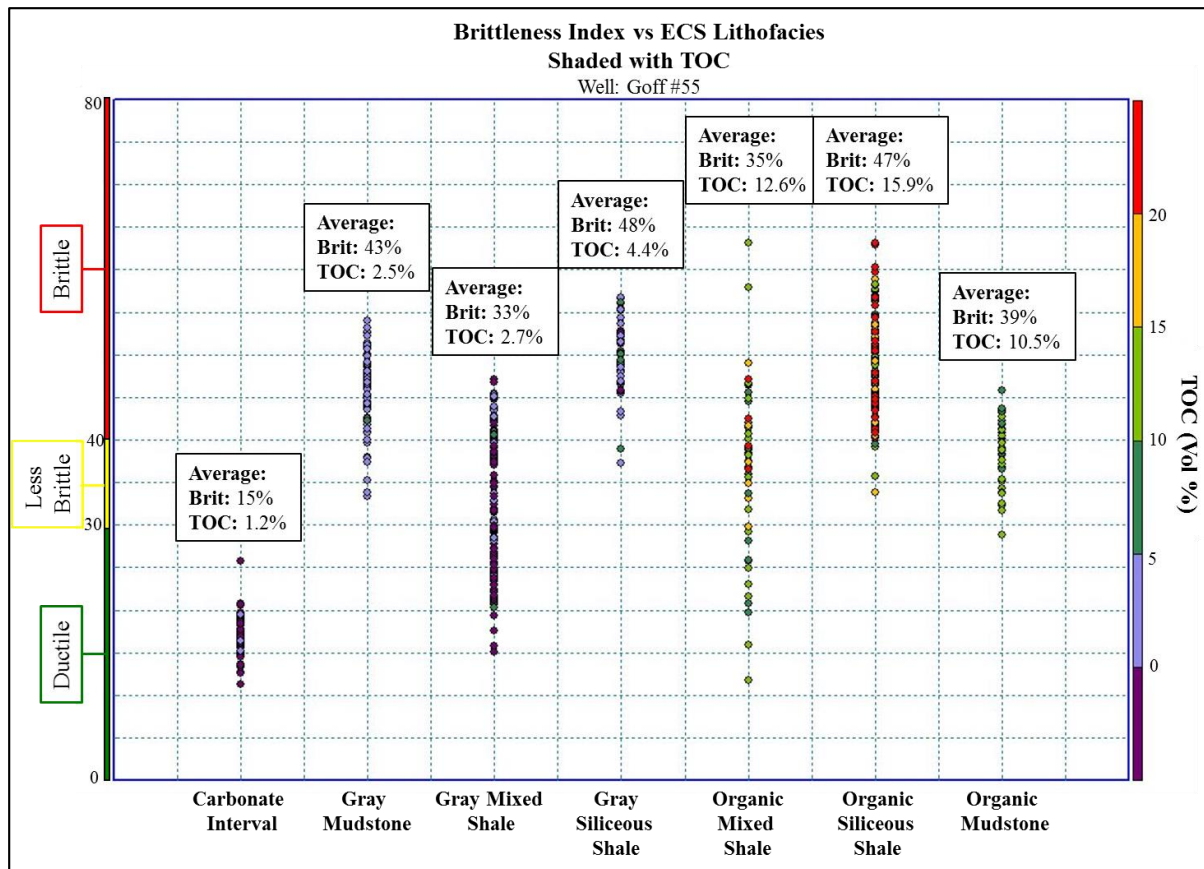


Figure 14. Cross plot of the ECS lithofacies versus brittleness computed using the brittleness index method, and shaded with volume percent TOC estimated using Schmoker's (1979) method.

ECS Lithofacies	Chlorite	Illite	Calcite	Pyrite	Quartz	TOC	Brit
Carbonate Interval	2.8	12.6	64.1	0.8	16.8	1.2	15.0
Gray Mudstone	9.6	35.1	2.0	0.6	44.1	2.5	43.0
Gray Mixed Shale	4.8	21.6	34.9	0.8	32.4	2.7	32.3
Gray Siliceous Shale	7.2	29.6	5.0	0.7	48.1	4.4	47.8
Organic Mixed Shale	1.9	20.0	29.1	1.6	29.8	12.6	35.0
Organic Siliceous Shale	3.9	29.4	3.3	2.2	41.7	15.9	47.0
Organic Mudstone	6.9	39.5	0.3	1.9	35.1	10.5	38.6

Table 1. ECS Lithofacies' average mineralogy as a volume percent and average estimated brittleness (Brit) computed by the brittleness index method.

Geomechanics:

While there is no universally accepted definition for brittleness, it can be generally defined as the rock's ability to crack or fracture with minimal or no plastic flow (Glossary of

Geology, 1960; Wang and Gale, 2009). The primary controls on brittleness include TOC, diagenesis, lithology, texture, fluid type, effective stress, temperature, and rock strength (references within Wang and Gale, 2009; Wells, 2004). For this research, brittleness was calculated using the brittleness average method proposed by Grieser and Bray (2007), and the brittleness index method proposed by Wang and Gale (2009).

The brittleness average method computes brittleness from Poisson's Ratio (Eq. 2) and Young's Modulus (Eq. 3) by normalizing and averaging both components (Eq. 4- 5) (Grieser and Bray, 2007). Poisson's Ratio is the amount a stretching a material will undergo due shortening/compression. Young's Modulus relates to the stiffness of a material. A low Poisson's Ratio and high Young's Modulus is associated with brittle materials, and the opposite is true for ductile materials (Grieser and Bray, 2007). Figure 15 is the cross plot of Poisson's Ratio and Young's Modulus shaded with the brittleness computed using the brittleness average method.

$$v = \frac{[0.5 \times (DTS/DTC)^2 - 1]}{\left(\frac{DTS}{DTC}\right)^2 - 1}$$

Equation 2. Poisson's Ratio (v) equation, where DTS is the shear sonic log and DTC is the compressional sonic log.

$$E = 2 \times (13400 \times Dens \div DTS^2) \times (1 + v)$$

Equation 3. Young's modulus (E) equation, where Dens is the rock density (g/cc).

$$v_{brittleness} = \frac{v - v_{max}}{v_{max} - v_{min}} \times 100 = \frac{v - 0.34}{0.14 - 0.34} \times 100$$

Equation 4. Equation to normalize Poisson's Ratio, where v_{max} and v_{min} are the minimum and maximum Poisson's Ratio measured.

$$E_{brittleness} = \frac{E - E_{min}}{E_{min} - E_{max}} \times 100 = \frac{E - 2.5}{6 - 2.5} \times 100$$

Equation 5. Equation to normalize Young's Modulus, where E_{max} and E_{min} are the minimum and maximum Young's Modulus measured.

The brittleness index method computes brittleness as a function of mineralogical composition (Eq. 6) (Wang and Gale, 2009). The equation proposed by Wang and Gale (2009) was adapted from Jarvie et al. (2007) equation to include dolomite and TOC. TOC will increase

ductility while dolomite, in addition to quartz, will increase brittleness (Wang and Gale, 2009). The brittleness computed by the brittleness index method is overlaid on the cross plot of Poisson's Ratio and Young's Modulus in Figure 16.

$$BI = \frac{Qtz + Dol}{Qtz + Dol + Ca + Cl + TOC}$$

Equation 6. Brittleness index (BI) equation, where Qtz is quartz, Dol is dolomite, Ca is calcite, Cl is clay, and TOC is total organic carbon.

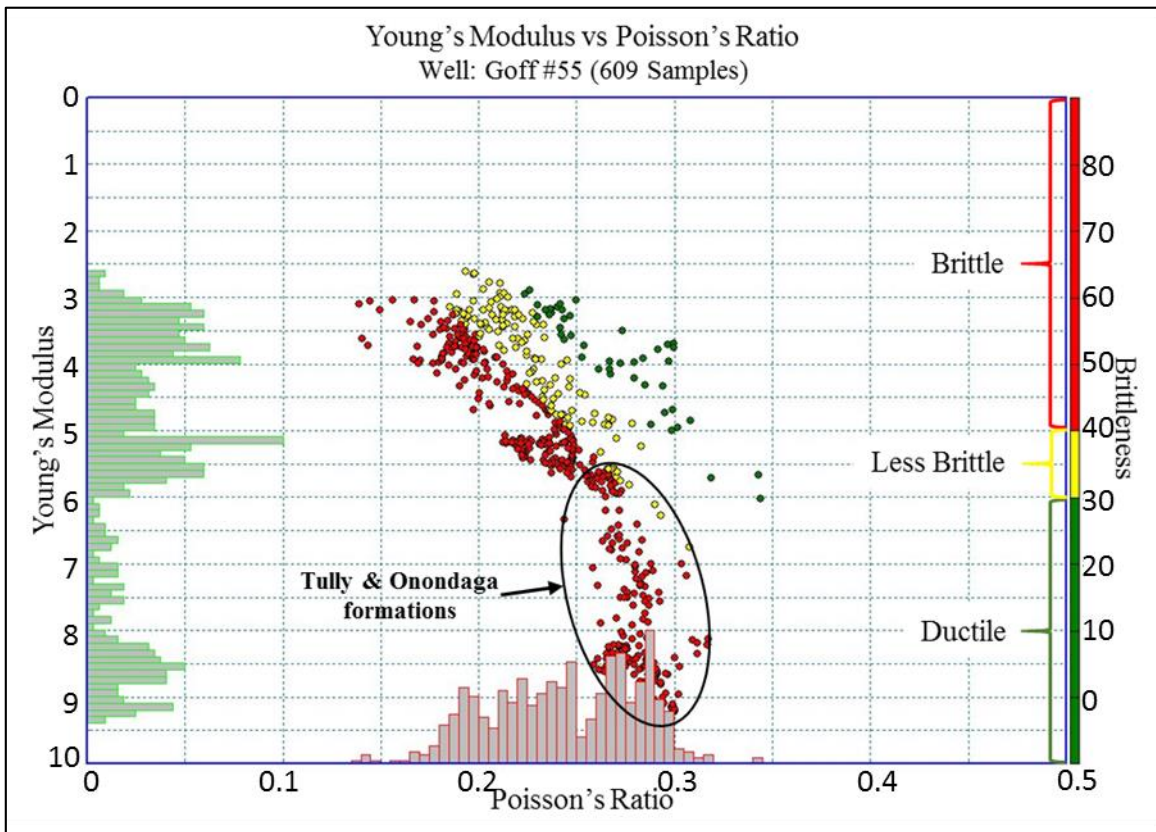


Figure 15. Cross plot of Poisson's Ratio and Young's Modulus shaded with the brittleness computed using the brittleness average method.

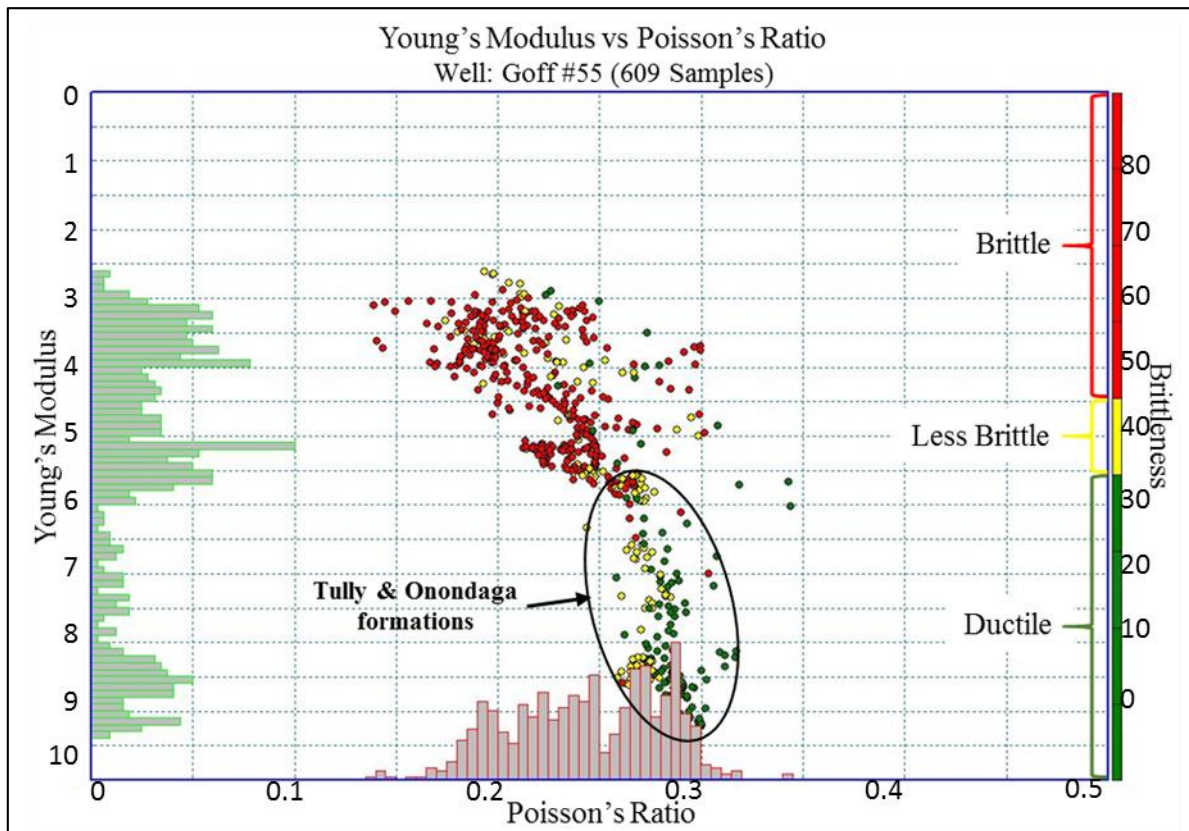


Figure 16. Cross plot of Poisson's Ratio and Young's Modulus shaded using brittleness computed by using the brittleness index method.

Physical Core:

The physical core was obtained from the core annex at the West Virginia Geological & Economic Survey, located off Mont Chateau Road in Morgantown, West Virginia. The depths of the core taken extended from 7,123ft – 7,235.75ft (112ft). These depths extend from two feet above the inferred Marcellus and Mahantango contact, and eight feet below the inferred contact between the Marcellus and Onondaga Limestone. The contacts were inferred from the well logs.

The core, which was partitioned into three-foot sections and placed in plastic bags inside cardboard boxes, was taken back to the laboratory. The boxes were laid out on tables in order of depth. Each plastic bag is marked with the core number, box/ bag number, and the upper and lower most depths at their corresponding end of the bag. At the end of each box is a lime green label with the company name, well name, field name, county and state, top and bottom depths of the core in the box, core number, and the box number. Each bag was checked to insure that it

corresponded with the box it was contained in. In the two cases where the bags were in the wrong box, they were moved to the correct box.

In order to ensure a more accurate description, a damp sponge was used to clean the driller's mud off of the flat faced side of the core. Along the left side of the core there is a vertical red line, the pieces of the core were checked to ensure that the red line was facing the left. If the line was on the opposite side, the piece would be flipped. By doing this, it ensured that every piece of the core was oriented in the correct vertical direction and not upside down. Also, every foot along the left side of the core is a yellow mark and the corresponding depth. These marks were used to help better constrain the depth measurements by placing a 12-inch ruler between them.

The rocks present in the interval of core that was described are predominately silty shales and some limestone intervals. The term silty shale was used as a general classification for the fine grained, siliciclastic rock composed predominately of silt-sized (1/16- 1/256mm) and clay sized (<1/256mm) particles (Boggs, 2012). If the unit was determined to be a limestone, it was classified according to depositional textures. The limestone was classified as a wackestone if it was a mud supported carbonate rock with more than 10% of the grains 0.3- 2mm in size, and a packstone if it was a grain supported, muddy carbonate rock (Boggs, 2012).

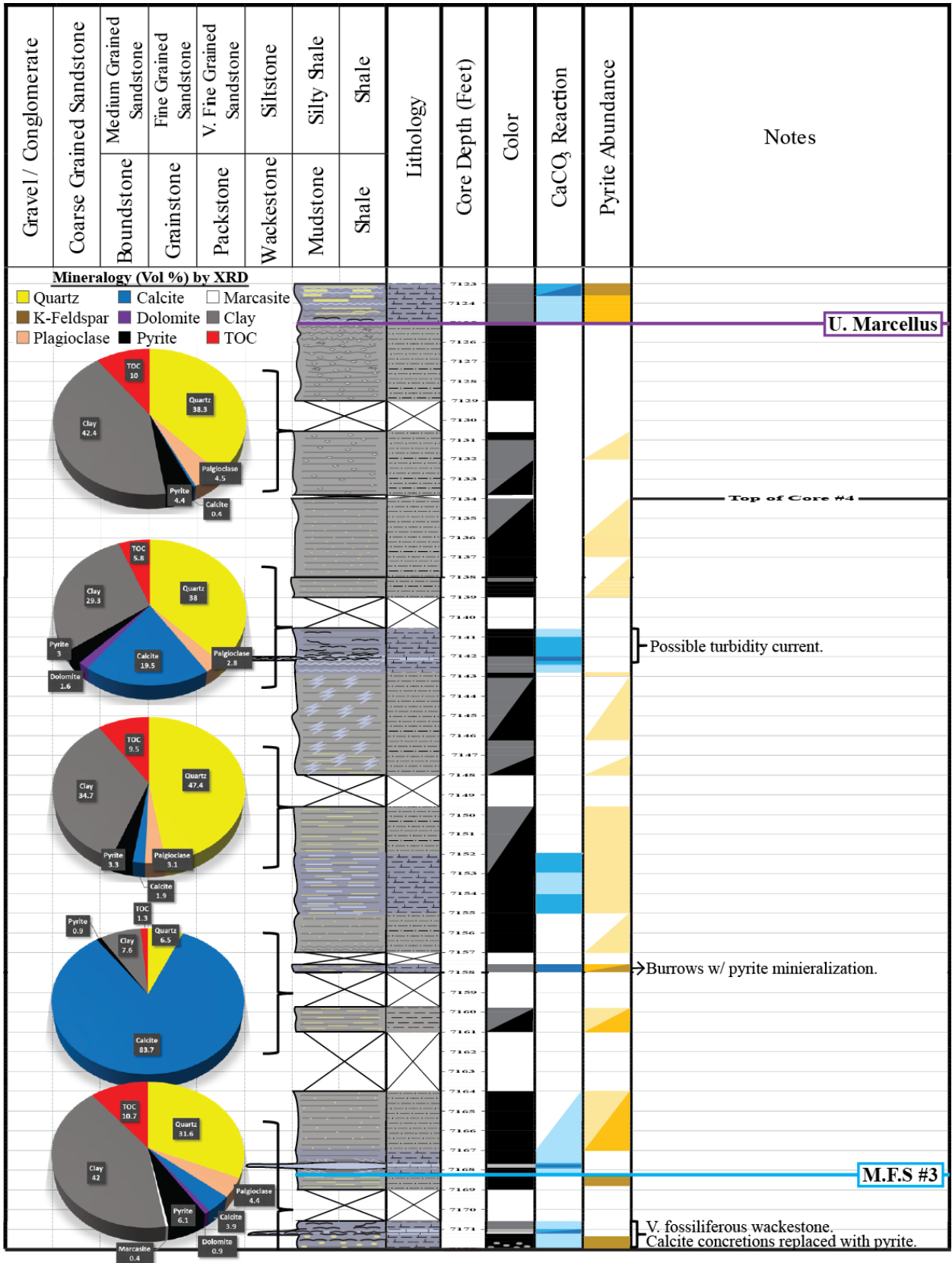
The core was described based on its physical characteristics. The main characteristics include color, bedding thickness, the presence or absence of rugosity along bedding planes, and dips of the beds. Bedding thickness was described as slabby (10- 30cm thick), flaggy (1- 10cm thick), and laminated (<1cm thick). While exact rose-compass orientation of the dip could not be given, the unit was said to be dipping to the right or left based on true vertical and the red line to the left.

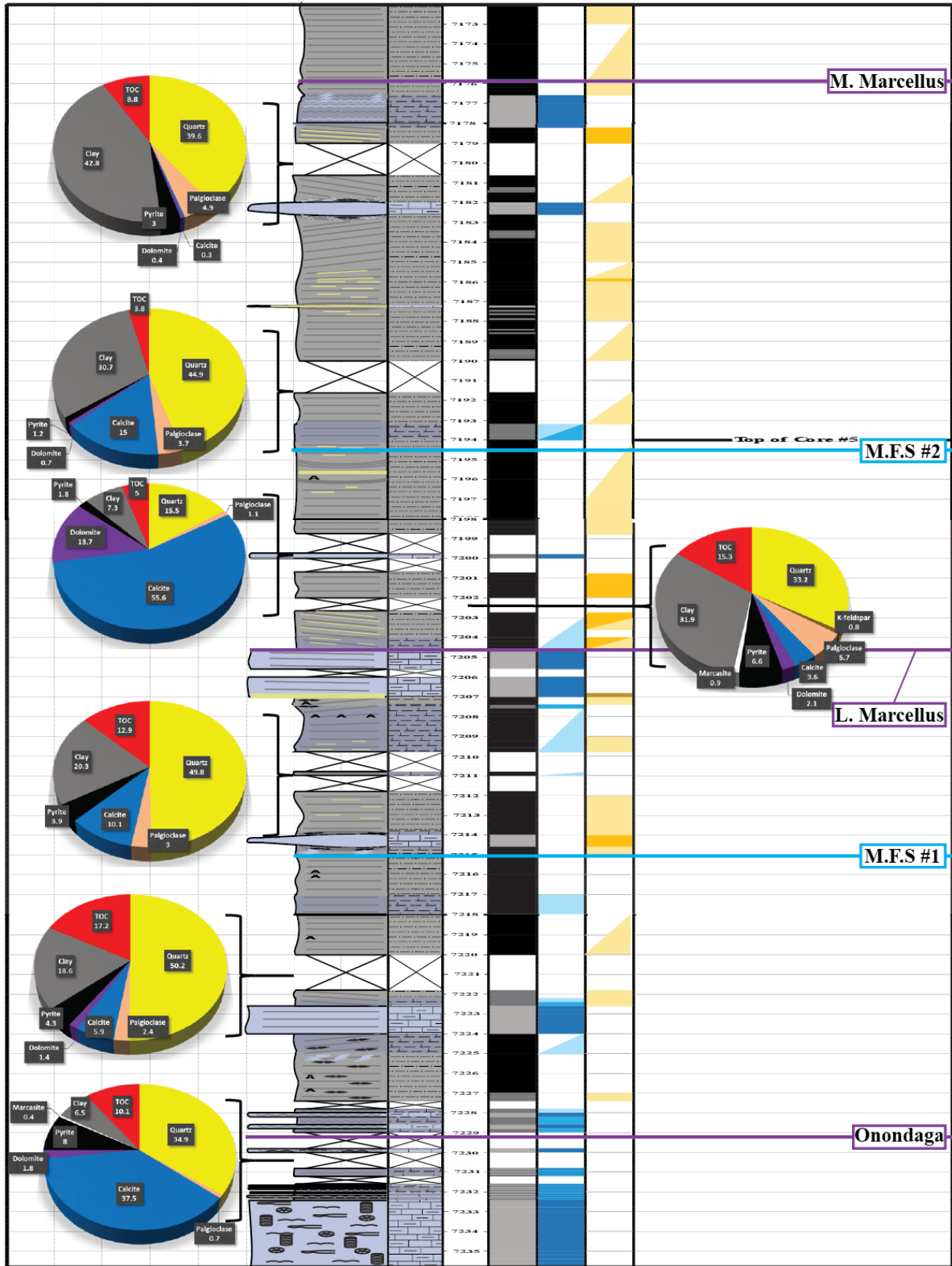
The core was also described based on the presence of calcite and pyrite. Hydrochloric acid was used to test for the presence of calcite. The abundance of calcite ranged from non-calcareous to very calcareous, and was based on the degree of effervescence. The acid was immediately wiped off with a damp sponge following the test. The abundance of pyrite was determined based on visual inspection, and had the same ranged from non-pyritic to very pyritic. If applicable, calcite and pyrite would be described as concretions, nodules, laminae, or relative crystal size.

Fractures were described based on orientation, thickness, length, shape, and open versus filled. The orientation was described in general terms of vertical, sub-vertical, horizontal, sub-horizontal, parallel or perpendicular to bedding, and if a dip could be estimated to the right or left it would be given. If the strike of the fracture was not relatively perpendicular to view, but rather parallel (trending left and right) then this would be specifically stated in the description. If the fracture was filled, the specific mineral filling the fracture would be determined.

Other properties described include the presence of fossils, ash beds, slickensides, and potential burrows. Fossils were described based on the abundance, the type or skeletal fragments if too broken, and if there were part of a turbidity sequence or strictly located along bedding planes. Ash beds were described based on color, texture, and size. A note was made if slickensides were present along bedding planes. Burrows were described based on abundance, color, and mineralogical composition. If a section of core was missing, this was noted.

The resulting core descriptions and pictures of the core are attached in Appendix I. The core descriptions, Ingrain's CoreHD[®] Whole Core High Definition CT Scanning movies, and XRD mineralogy reports were used to make a stratigraphic column in Adobe Illustrator CC (Figure 17). The stratigraphic column is scaled such that it can be plotted next to well logs of the same scale so that accurate comparison can be made between the different parameters (Figure 18).




















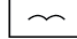





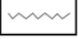





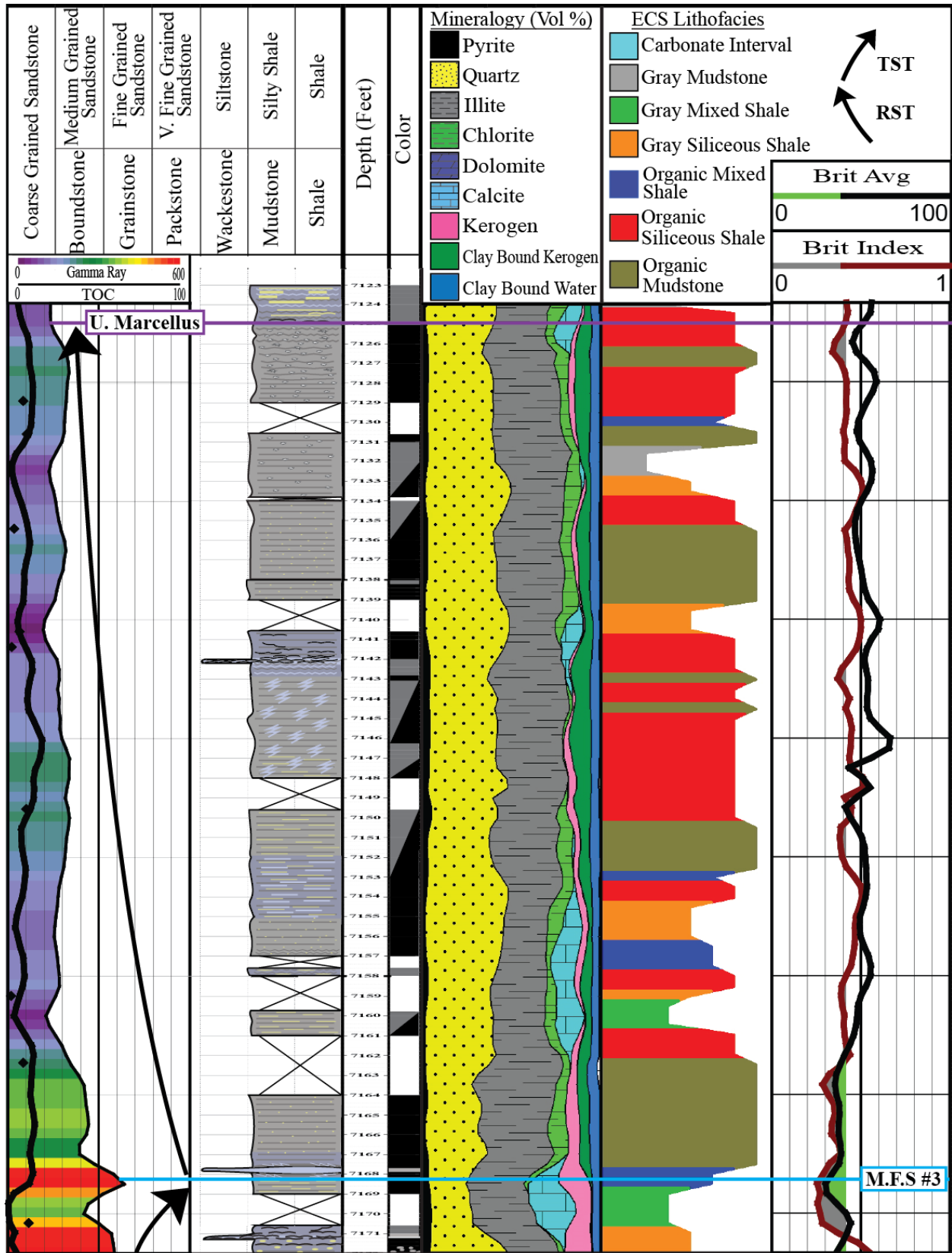
<u>Stratigraphic Column Explanation:</u>			
<u>Lithology</u>	<u>Core Color</u>	<u>Calcite Abundance</u>	<u>Pyrite Abundance</u>
 Silty Shale	 Light Gray	 None	 None
 Calcareous Shale	 Medium Gray	 Slightly	 Slightly
 Argillaceous Shale	 Black	 Moderately	 Moderately
<u>Symbols</u>	 Ash Bed	 Very	 Very
 Brachiopod	 Slickensides	 Planar Bedding	 Pyrite Laminae
 Crinoid	 Calcite filled Fracture	 Crinkly Bedding	 Calcite Laminae
 Echinoderm	 Pyrite Nodules	 Maximum Flooding Surface	 Tops

Figure 17. The resulting stratigraphic column made using core descriptions, Ingrain's CoreHD® Whole Core High Definition CT Scanning movies, and XRD mineralogy reports. The tops for Upper (U.), Middle (M.), and Lower (L.) Marcellus and Onondaga are plotted in purple. The tops for the maximum flooding surfaces (M.F.S) 1 -3 are plotted in blue.



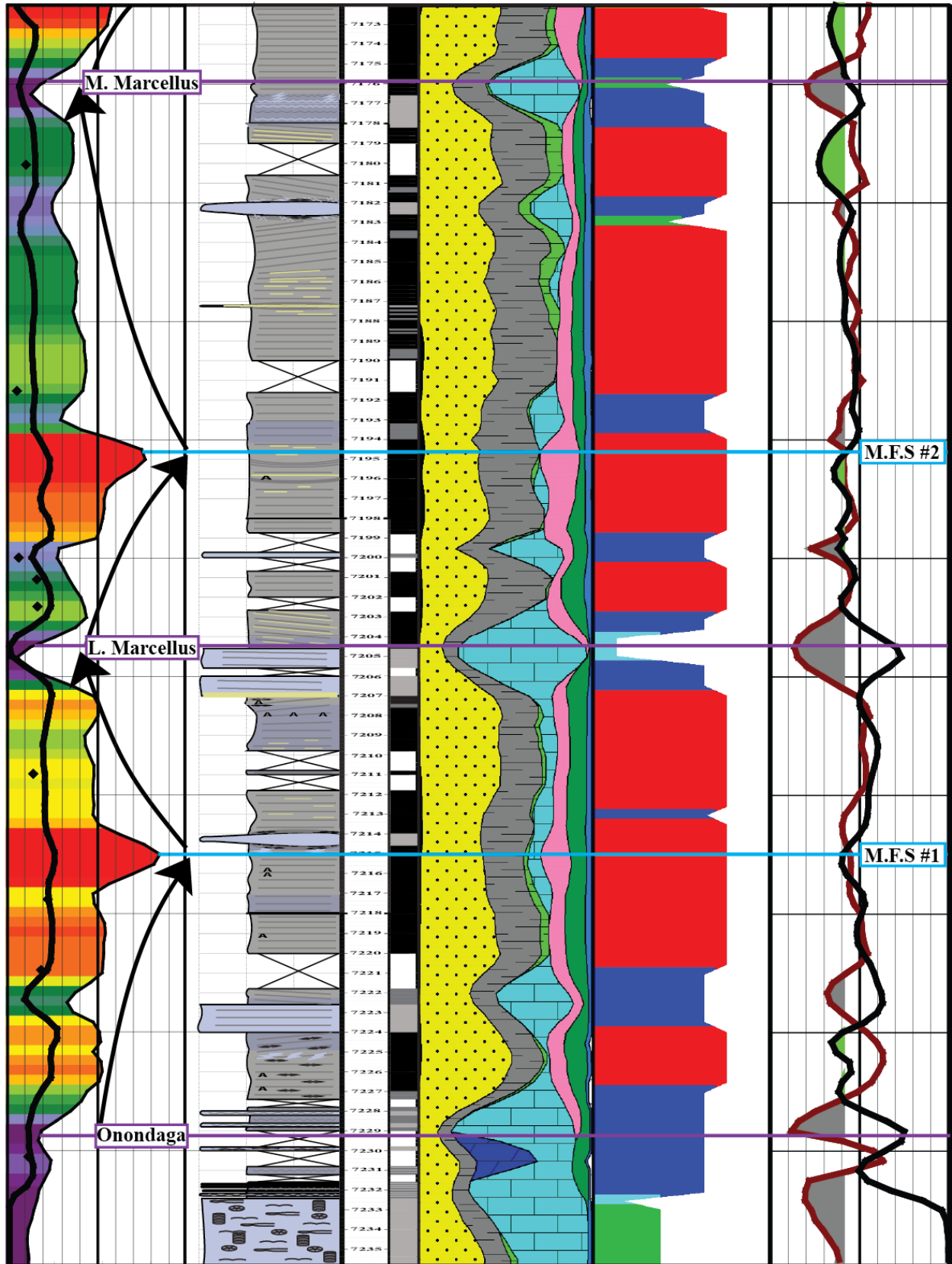


Figure 18. The scaled stratigraphic column and well logs are plotted next to one another for easy comparison of the different parameters. In Track 1 gamma ray is plotted (0-600 API) and shaded using Geo-column shading. Total organic carbon (TOC) was estimated using Schmoker's (1979) equation, and is plotted as a volume percent (0-100%). Measured TOC from pyrolysis, and 2D SEM analysis is plotted as black diamonds. Arrows representing transgressive system tracts (TST) and regressive system tracts (RST) are next to the gamma ray log. The stratigraphic column, depth scale, and core color column are plotted between tracks one and two. In Track 2 ELAN mineralogy plotted as a volume percent (0-100%). The predicted lithofacies plotted in Track 3 were computed using ELAN mineralogy, estimated TOC, and the classification scheme proposed by Wang (2012). The brittleness average and brittleness index is plotted in Track 4, and shaded to show when brittleness is less than 40 (the less brittle to ductile zone). The Marcellus and Onondaga Limestone tops are plotted in purple, and maximum flooding surfaces (M.F.S) in blue.

Regional Sequence Stratigraphy:

A regional sequence stratigraphy was developed surrounding the study well using available well log data from approximately 40 wells. The gamma ray log was the primary log used to develop the sequence stratigraphy. If available, correlation was aided by bulk density, neutron porosity, and density porosity. Gamma ray was the primary log used due to the fact that it was the only log available for most wells in the area.

The tops chosen for the Goff #55 well were extrapolated to surrounding wells. Map 1 displays the well location of wells with any of the fore mentioned logs in West Virginia. The tops correlated across the area were for the Onondaga Limestone, the three tops picked for the Marcellus Formation based on T-R sequences, and the tops for the Mahantango and Tully formations. A finer scale sequence stratigraphy for only Harrison County, WV could not be developed due to the scarcity of wells with available logs. Therefore, a coarser scale sequence stratigraphy was developed for Harrison County and the surrounding counties in north central and mid-central West Virginia (Fig. 19- 25).

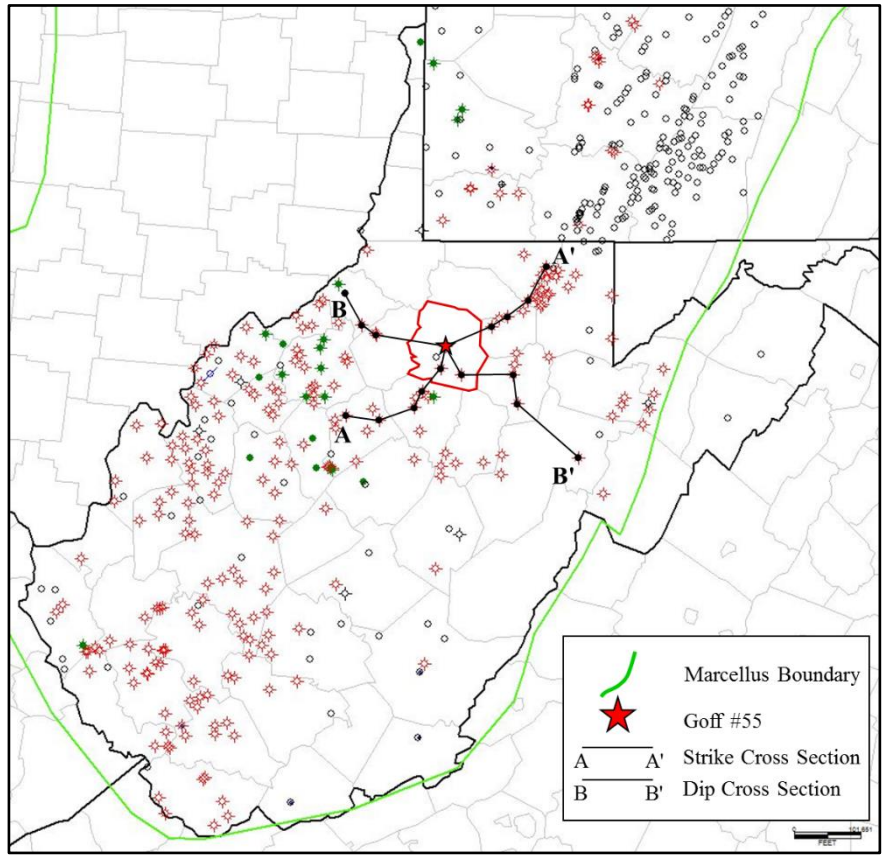


Figure 19. Map of West Virginia showing wells with gamma ray, bulk density, neutron porosity, or density porosity logs. Harrison County, WV is outlined in red.

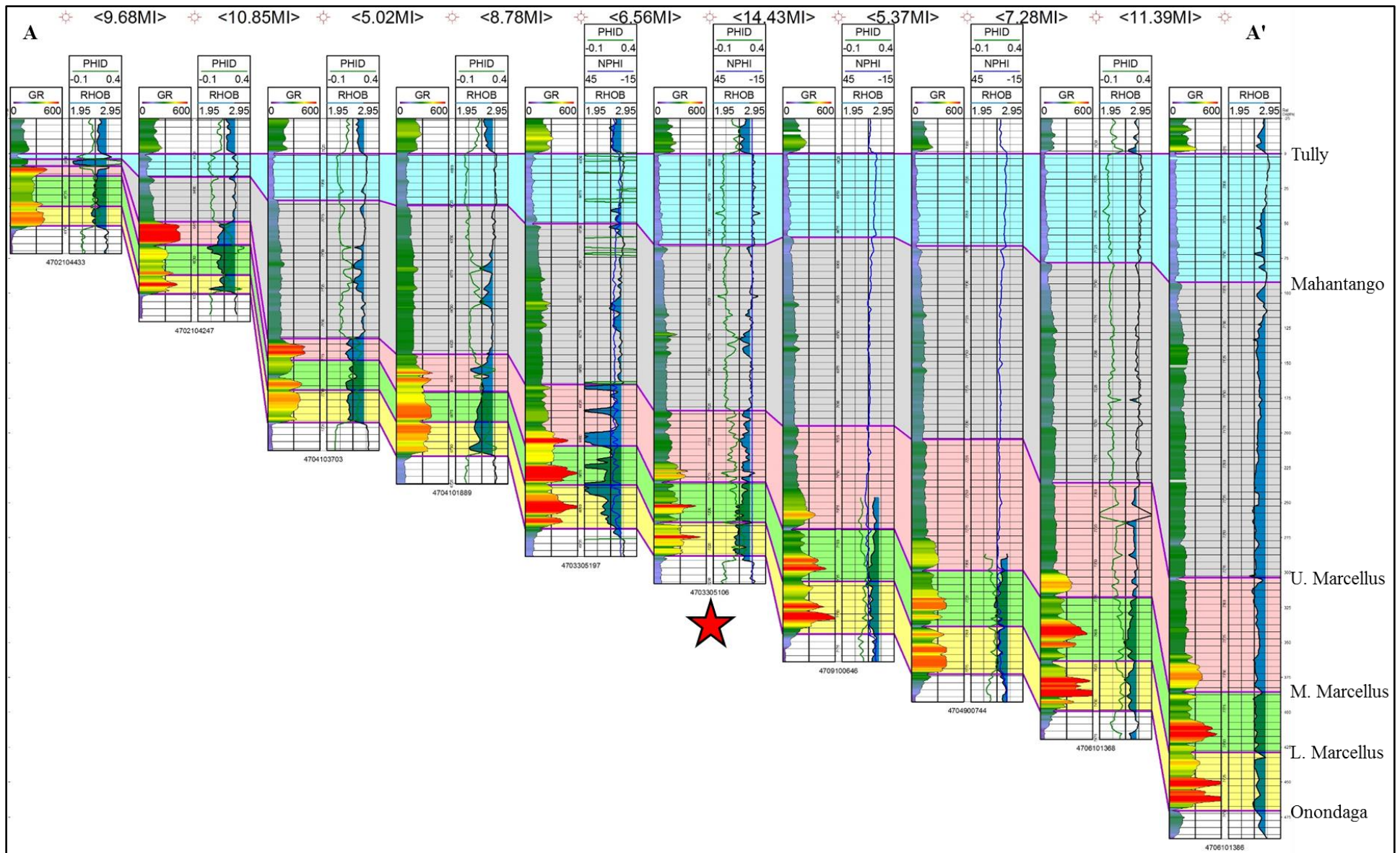


Figure 20. Along strike cross section (A- A') flattened on the top of the Tully Formation. The cross section extends from 25 feet above the Tully Formation to 25 feet below the Onondaga Limestone top. The Goff #55 well is denoted by the red star.

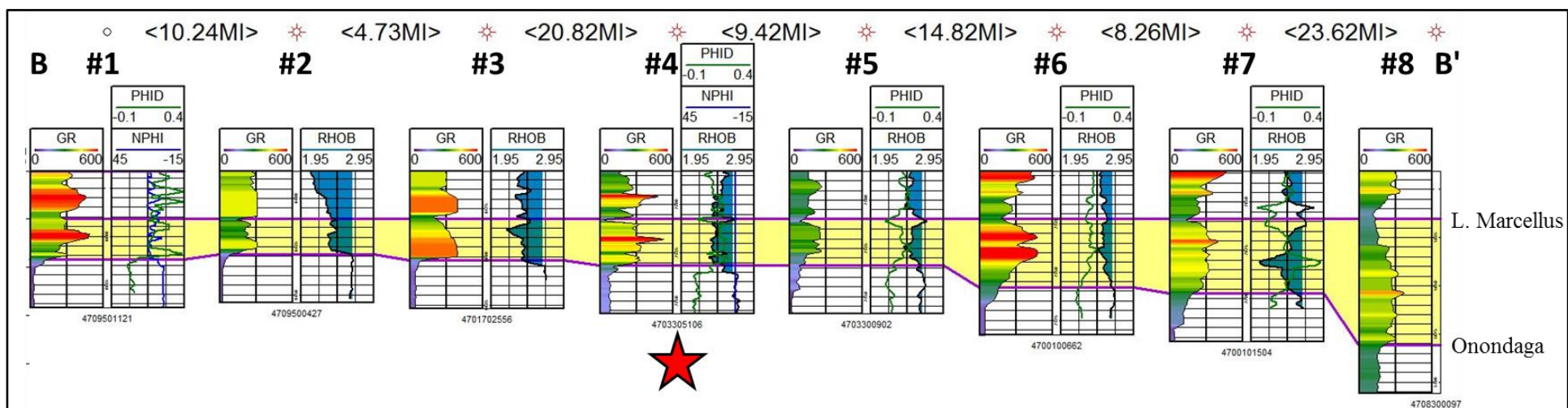


Figure 21. Down dip cross section (B- B') flattened on the top of the lower (L.) Marcellus. The cross section extends from 25 feet above the L. Marcellus top to 25 feet below the Onondaga Limestone top. The Goff #55 well is denoted by the red star.

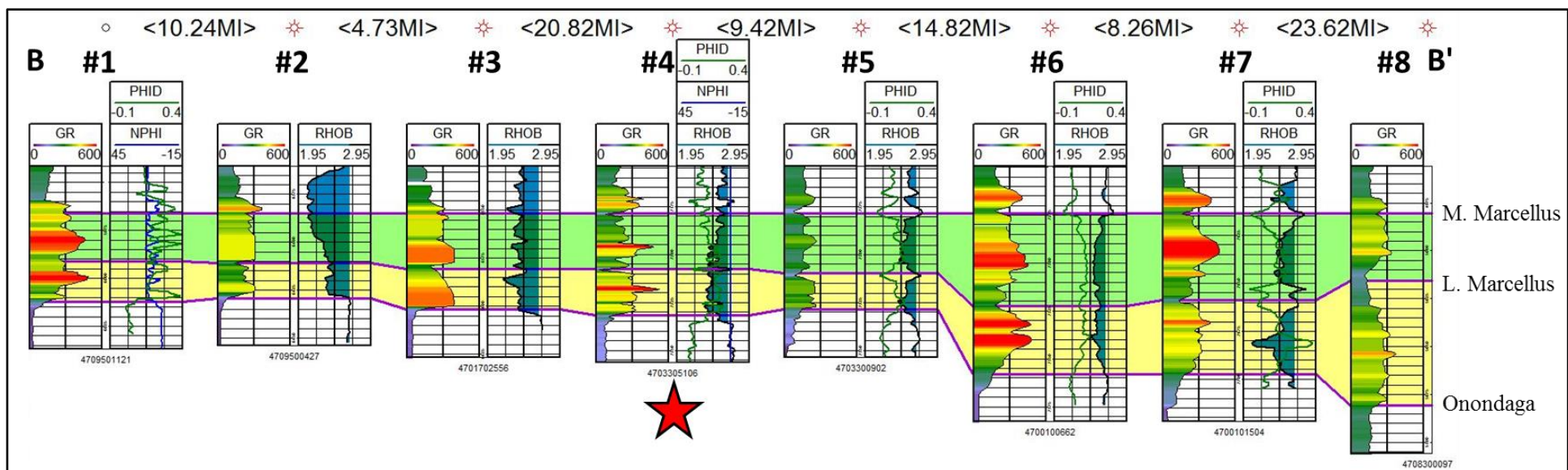


Figure 22. Down dip cross section (B- B') flattened on the top of the middle (M.) Marcellus. The cross section extends from 25 feet above the middle Marcellus top to 25 feet below the Onondaga Limestone top. The Goff #55 well is denoted by the red star.

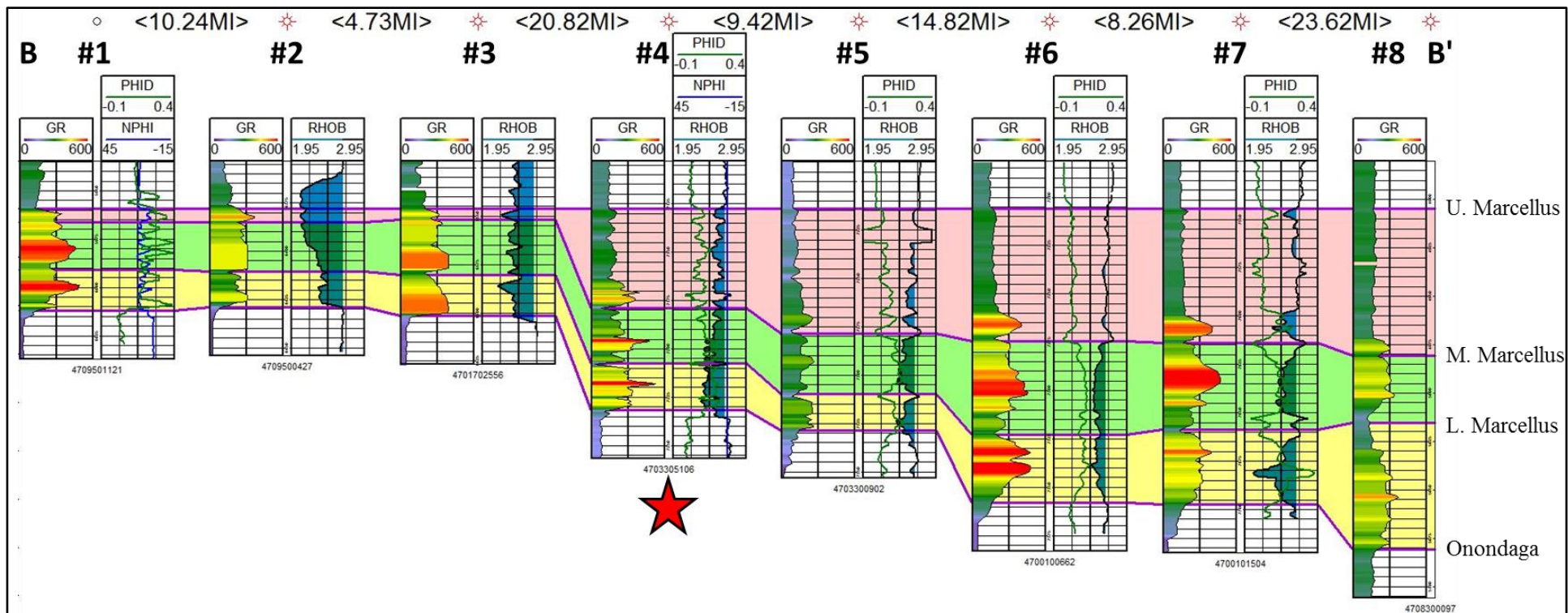


Figure 23. Down dip cross section (B- B') flattened on the top of the upper (U.) Marcellus. The cross section extends from 25 feet above the U. Marcellus top to 25 feet below the Onondaga Limestone top. The Goff #55 well is denoted by the red star.

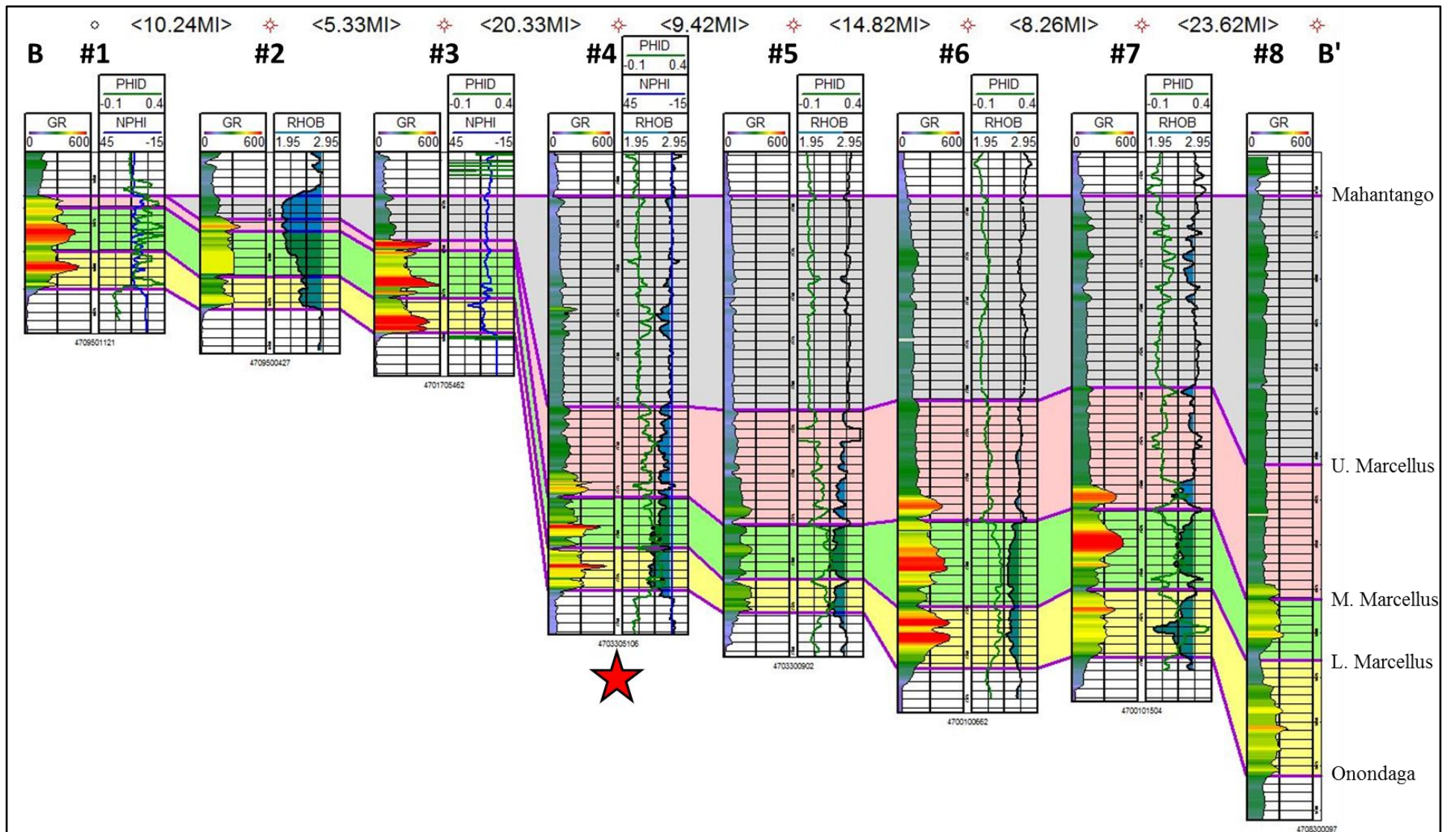


Figure 24. Down dip cross section (B- B') flattened on the top of the Mahantango. The cross section extends from 25 feet above the Mahantango Formation top to 25 feet below the Onondaga Limestone top. The Goff #55 well is denoted by the red star.

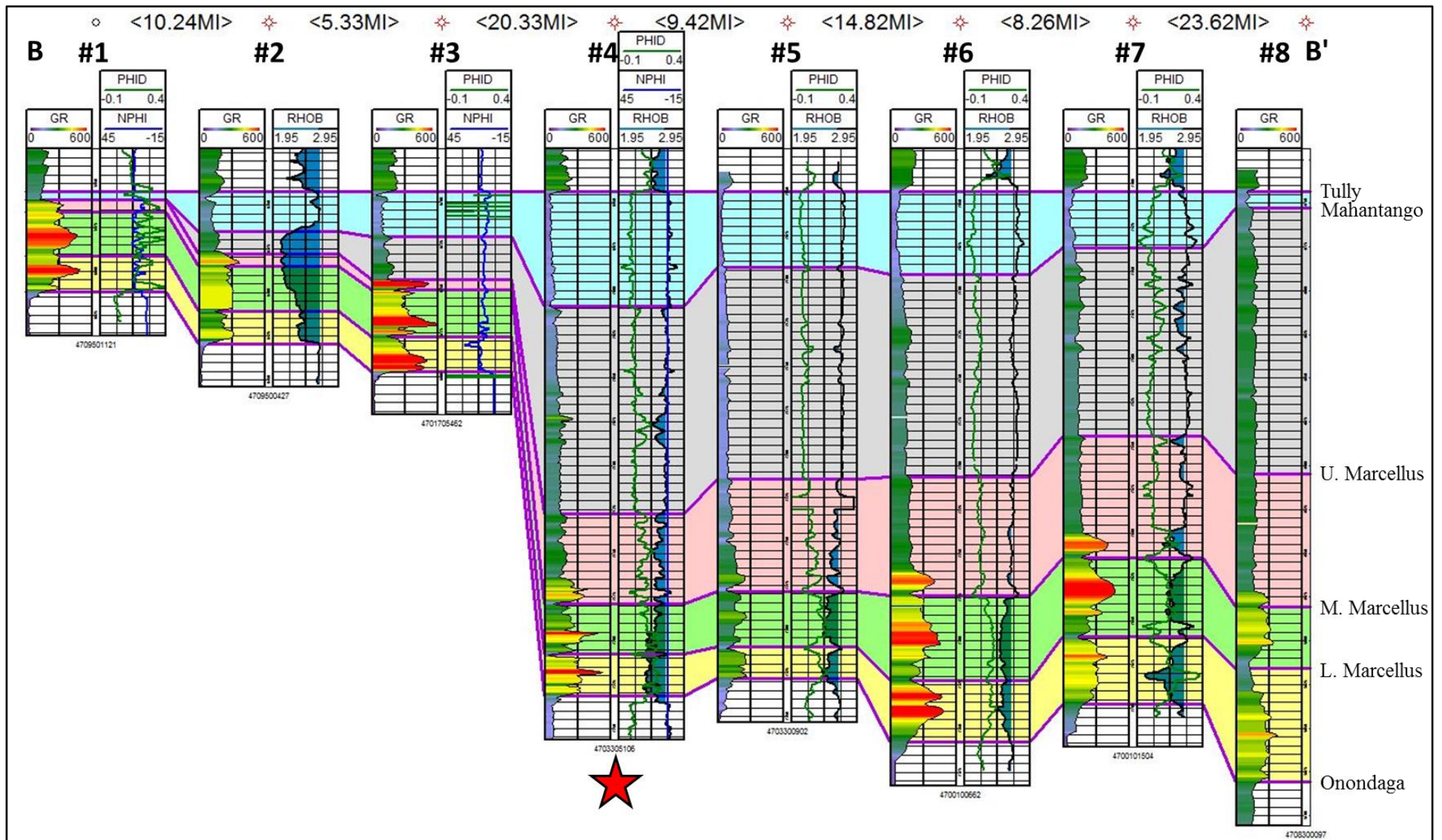


Figure 25. Down dip cross section (B- B') flattened on the top of the Tully. The cross section extends from 25 feet above the Tully Formation top to 25 feet below the Onondaga Limestone top. The Goff #55 well is denoted by the red star.

DISCUSSION:

TOC & Pyrite:

Overall, the Marcellus Formation's organic richness increases with depth. The lower Marcellus is the most organically rich interval in the formation. The amount of TOC present in the formation was estimated using the density log, and had an 81% correlation with the laboratory measured TOC values (Fig. 7). This is a significant enough correlation that the derived values can be used as an accurate representation of the amount of organic matter present for the formation.

In the cross section of Goff #55 the bulk density log was shaded to show when the density dropped below 2.65g/cc (Fig. 6). This was done because of the inverse relationship that exists between TOC and the density of sedimentary rock. TOC drops to almost zero once rock density reaches 2.65g/cc or higher (Fig. 8). The outlier present in the data may have been due to errors during laboratory testing, well log measurement, or a reflection of the resolution limits of the density tool. This relationship can be used as a quick visual proxy for the presence of organic matter, but must not be used as the sole proxy for TOC.

There is a direct relationship between TOC and pyrite (Fig. 9). Based on XRD values taken from the core there was an 80% correlation between pyrite and TOC. The presence of pyrite in shale is indicative of a reducing benthic environment which is preferable for organic matter preservation (Lash and Blood, 2014; Castle, 2001). This relatively strong and direct correlation indicates that preservation was mostly due to the dysoxic to anoxic conditions. Some of the lack of correlation could be due to increased clastic influx into the basin causing organic matter degradation and/or dilution (Lash and Blood, 2014). This clastic influx model would explain points where there are high amounts of pyrite present but low amounts of TOC (Fig. 9). These points could also be explained by a decrease of productivity in surface water due to a lack of nutrients. There is also the possibility of pyrite replacement occurring after burial and not being intimately related to the depositional environment.

In addition to the relationship pyrite had with TOC, there was also a strong relationship between Pyrite and the T-R sequences (Fig. 26). The pyrite mineralogical log could be used to

assist in separating the Marcellus Formation into different units based on T-R sequences. Pyrite abundance would increase during a RST and fall during a TST. This indicates that when sea level rose during the RST there would be stronger reducing conditions present. Bottom water anoxia was possibly enhanced when sea level rose due to the decreased ability for the water column to mix.

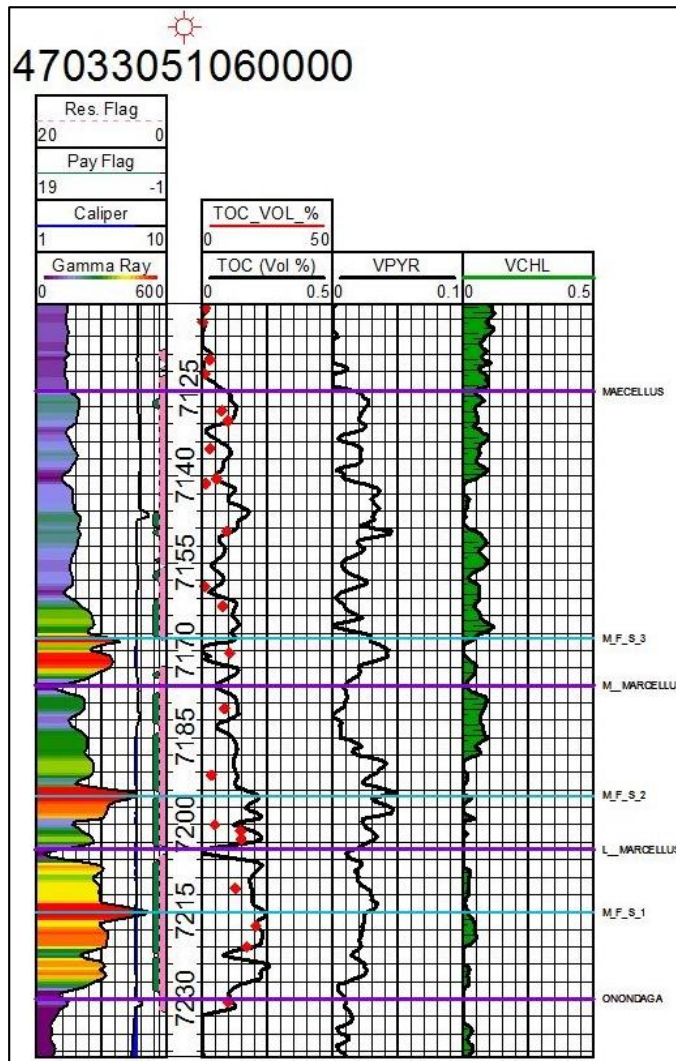


Figure 26: Cross-section of the Goff #55 study well. Plotted in Track 1 is the reservoir (Res) flag, pay flag, caliper log shaded for values less than 7.875 inches, and gamma ray log. In Track 2 are core measured TOC values (volume %) plotted as red diamonds, and the estimated TOC log. In Track 3 is the mineralogical log of pyrite in volume percent (VPYR). In Track 4 is the mineralogical log of chlorite in volume percent (VCHL).

Geomechanics:

When comparing the cross plots for the brittleness average method (Fig. 15) and brittleness index (Fig. 16) method there was a noticeable discrepancy in brittleness between the two methods for the Tully and Onondaga limestones. For the brittleness average method, the

Tully and Onondaga limestones were characterized as brittle (Fig. 15). However, the brittleness index method classified the two limestone formations as ductile to less brittle (Fig. 16). These two methods also conflicted for the smaller carbonate rich layers present within the Marcellus Formation. From the Poisson's Ratio and Young's Modulus cross plot shaded with the ECS Lithofacies it is clear that this discrepancy is predominately in the carbonate intervals and gray mixed shales (Fig. 27). The characterization of brittleness for the other lithofacies have a better correlation between the two methods.

When the two logs are plotted against one another using the same scaling there are similarities that are not readily noticeable in the cross plots (Fig. 18). Ignoring the fore mentioned contradiction between the two methods for the calcite intervals, they generally predict similar brittleness for the other facies throughout the Marcellus Formation. The two methods crisscross, overlap, and stay within a few units of each another. The best example of this agreement between the two methods is from 7,163 -7,170ft (Fig. 18). Both methods are predicting the interval to be ductile, and both curves have a very similar shape. From 7,124 - 7,143ft the curves do not overlap but rise and fall with relative unison with one another.

There were two organic siliceous shale intervals, at 7,173ft and 7,180ft, that the brittleness average method estimated to be ductile while the brittleness index method predicted the intervals to be brittle (Fig. 18). While most siliceous shale is brittle because of the increase in silica these two intervals also have a fair amount of chlorite. Chlorite and illite are the two clay minerals decomposed by the Spectrolith[®] mineralogical log. Intervals and wells with high amounts of chlorite are harder to fracture and worse producers due to an increase in ductility induced by the chlorite minerals. Therefore, the characterization of these two intervals as ductile by the brittleness average method may not be completely inaccurate. Laboratory testing is needed to either confirm or reject the results for these intervals.

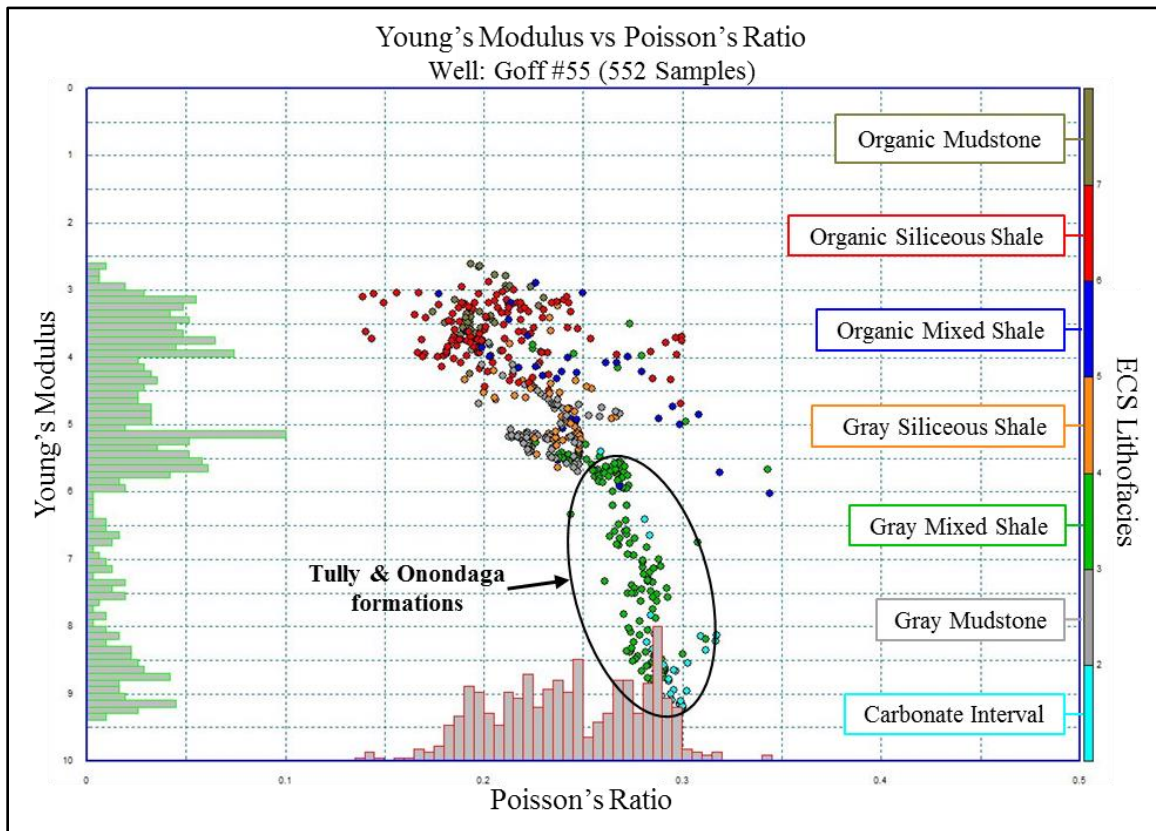


Figure 27. Cross plot of Poisson's Ratio and Young's Modulus shaded by ECS Lithofacies.

ECS Lithofacies:

The shale lithofacies computed the using the ELAN mineralogical logs are not as fine scaled as the actual core description, but serve as an accurate representation of the reservoir for the purpose of drilling or fracturing. In some ways they prove more beneficial than the descriptions of the physical core. When describing the core it is difficult to tell when a shale becomes more siliceous rich vs mudstone rich and the ratio between quartz to carbonate. The ECS lithofacies also tie the mineralogy with TOC so the organic rich intervals are easily discernable.

The relationship between the ECS lithofacies and the stratigraphic column were consistent with one another (Fig. 18). The ECS lithofacies cannot resolve the limestone beds less than a foot and a half, but it does classify these beds and the surrounding shale as mixed shale lithofacies. The areas of the core that were described as shale and moderately to very

effervescent in the presence of diluted hydrochloric acid were also characterized as mixed shale ECS lithofacies. The gray shale facies, which are non-organic, corresponded to shale intervals of the physical core that were described as having a grayish color.

Hydrocarbons associated with organic matter and increased brittleness due to silica content and lower amounts of clay and carbonate minerals make intervals with abundant organic siliceous shale a primary completion target in the Marcellus Formation (Fig. 14) (Wang, 2012; Singh, 2008). The organic siliceous shale lithofacies had an average TOC of 16%. This was the highest TOC average of all the lithofacies; of the three organic facies it had the highest predicted average brittleness (47%) (Fig. 14). The only facies that had a higher estimated brittleness than the organic siliceous shale was the gray siliceous shale. This is to be expected since the presence of organic matter serves to increase ductility.

Organic mixed shale lithofacies had the second highest average organic content (12.6%). However, out of the seven facies the organic mixed shale had the third lowest estimated brittleness (35%) (Fig. 14). The two facies with a lower estimated brittleness were the gray mixed shale and carbonate intervals, respectively. The increased presence of calcite decreases the brittleness of a rock. The organic mixed shale is a secondary target because the increased abundance of carbonate is not as conducive to the propagation of fractures as the silica in the organic siliceous shale.

The organic mixed shale's counterpart, the gray mixed shale facies, was less brittle because of increased calcite abundance and clay minerals (particularly chlorite). When compared to the organic mixed shale, the gray mixed shale had a 6% increase in clay and calcite, a 10% decrease in TOC, and 1.5% increase in quartz (Table 1). This indicates that calcite and clay have a greater effect on brittleness than TOC. This was the only facies where the non-organic facies was predicted to be less brittle than the organic.

Of the three organic facies the organic mudstone had the lowest estimated TOC (10.5%), and it had an estimated brittleness of 39%. While the organic mudstone facies had over 40% clay minerals, it also had a fair amount of quartz (35%) which contributed to its brittleness (Table 1). It had more quartz than either the mixed shale facies or the carbonate intervals, which, in addition to the lack of calcite, is why it was estimated to be more brittle than those two

lithofacies. The gray mudstone was estimated to have a higher brittleness than the organic mudstone because of a greater abundance of quartz and less organic matter.

The gray siliceous and mixed shales are not completion targets due to very low amounts of organic material, averaging 4.4% and 2.7% respectively. However, they could serve to stimulate fracture growth and connect the borehole to the primary targets (Wang, 2012). The carbonate intervals are not conducive to fracture propagation, and can be utilized to control fracture growth. Due to high clay content, increased ductility, and minimal amounts of TOC (2.5%) the gray mudstone should be avoided.

The upper, middle, and lower Marcellus had varying percentages of the different lithofacies present (Fig. 13). These changes agreed accordingly with a T-R sequence model. The lower and middle Marcellus were the most similar with little difference in lithofacies percentages. The upper Marcellus was the most different and diverse in facies.

Marcellus Formation:

The Marcellus to Tully Formation is one large, 2nd order T-R sequence. The organic rich shale of the Marcellus Formation is the TST, and the coarsening upward through the upper half of the Marcellus Formation, the Mahantango Formation, and to the fossiliferous limestone of the Tully Formation is the RST. Unlike Lash and Engelder's (2011), this study divided the Marcellus Formation into three 3rd order T-R sequences instead of two (Fig. 11). The T-R sequences formed as a result of the interplay between sea level change, flexural subsidence, and sediment supply.

The discrepancy in the amount of 3rd order cycles within the Marcellus Formation may be due to top placement. There is some debate amongst scientist as to where exactly the Marcellus Formation ends and the Mahantango Formation begins. While both formations are shale, the Mahantango is characterized as a non-organic shale as opposed to the organic rich Marcellus Formation. This characterization of the two formations was yielded to when choosing the top for the Marcellus Formation.

While some chose to place the Marcellus formation top directly on the last hot shale gamma ray signature, this study chose to place it at the point where there was no longer any

indication of TOC present. By choosing this placement method there was a clear third T-R sequence present in the Marcellus Formation. When the top was compared to core it directly correspond to a point immediately below a shale that was heavily burrowed. These burrows indicate that the water column had become oxygenated enough to support organisms, and ultimately destroy the preservation potential of organic matter.

When two 2D scanning electron microscope (SEM) images within a few feet on either side of the Marcellus Formation top were compared there was a noticeable difference in the rock lithology (Fig. 28 & 29). The main difference was the lack of pyrite framboids and organic matter present in the SEM image of the Mahantango Formation. Pyrite framboids are present in reducing environments, therefore, the lack of them further serves as an indication of an oxygenated water column.

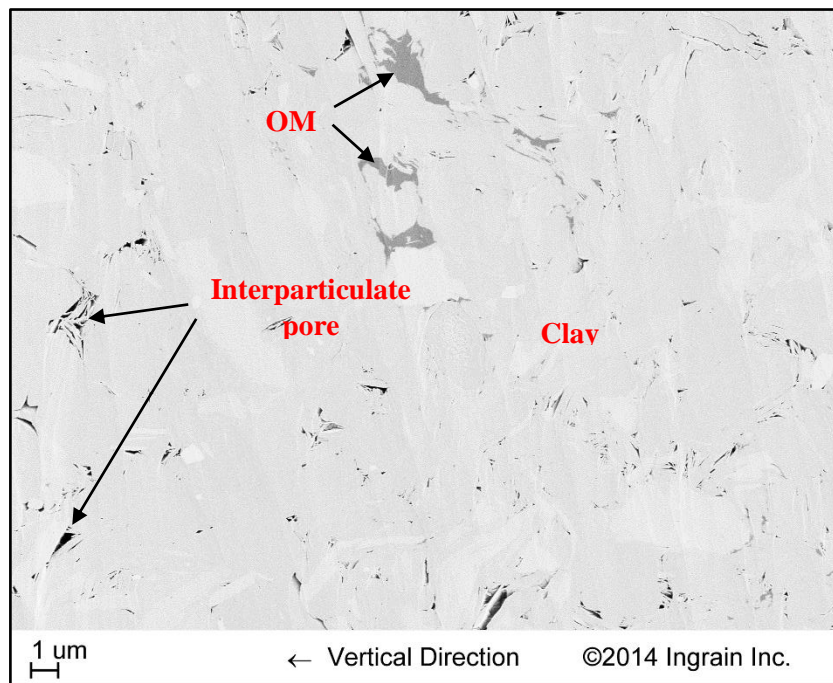


Figure 28: 2D SEM image taken of the core at 7,122ft. The sample was taken from the Mahantango Formation, and located approximately 3ft (1m) above the Marcellus Formation Top.

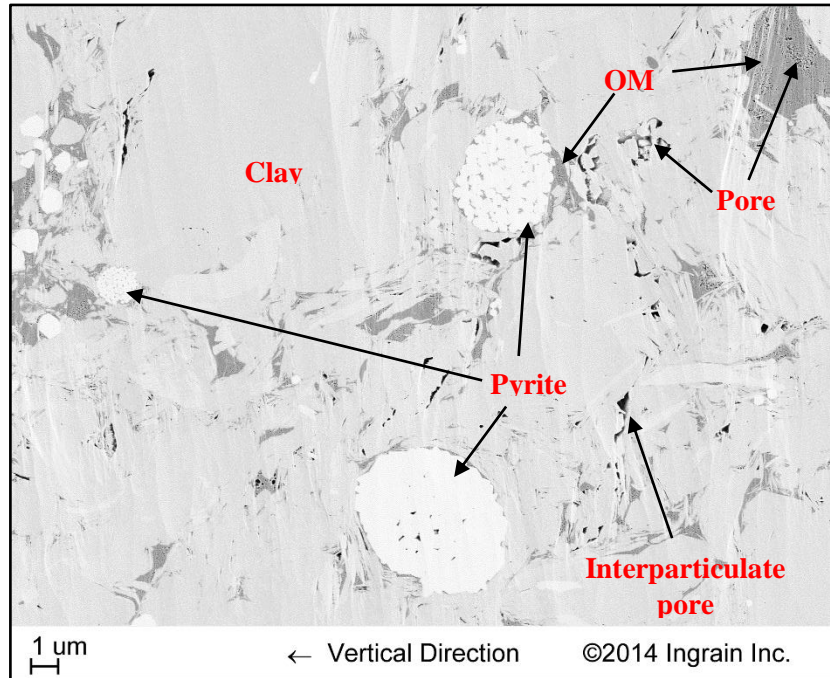


Figure 29: 2D SEM image taken of the core at 7,128ft. The sample was taken from the Marcellus Formation, and located approximately 3ft (1m) below the Marcellus Formation Top.

Lower Marcellus:

In the basin, the lower Marcellus is typically the better producing interval and more highly targeted for drilling. It had the highest estimated TOC average at 18.7% by volume. The explanation for the increased production can be sought after by examining the ECS Lithofacies and their stacking patterns. The lower Marcellus was composed of 66% organic siliceous shale, 30% organic mixed shale, and 4% carbonate intervals (Fig. 13). The carbonate interval was at the very top of the lower Marcellus at the end of the RST (Fig. 18). There are only seven facies changes present in the lower Marcellus; the facies are clumped together. Most of the organic siliceous shale is in the middle to upper portion of the unit. There is a 10ft and 6ft section of organic siliceous shale separated by a 0.5ft interval of organic mixed shale. This half foot interval of organic mixed shale is a calcite concretion, and is not thick enough to truly affect fracture propagation. Therefore, it can be ignored and the two sections of organic siliceous shale can be considered one thick, continuous interval. The two organic mixed shale intervals at the base sandwich a 2.5ft thick organic siliceous shale. The organic mixed shale intervals are estimated to be ductile and would hinder fracture growth.

As previously mentioned, in the study well the transition from the Onondaga Limestone to the Marcellus Formation was gradational over an interval of four feet. The gradation was composed of interlayered beds of limestone and shale that eventually gave way to shale. The depositional environment during that time alternated between sub- to anoxic waters and oxygenated waters. The limestone was deposited during oxygenated periods where there was enough oxygen to support organisms. The thinning of the limestone beds and thickening of the shale beds indicate that the basin was becoming more prone to suboxic conditions. This was probably caused by the deepening of the basin to a depth where the destruction of reducing conditions is not as easily accomplished and would require greater fluctuations in sea level.

When examined in core, the shale throughout the lower Marcellus was black and there were centimeter scale pockets of ash present (Fig. 30). These little pockets of ash were commonly light gray with yellow staining and gritty in texture. They were more resistant to compaction than the surrounding shale and resulted in the shale breaking along bedding planes parallel to the ash. Finding pockets of ash and thin ash beds in the Marcellus Formation is not an uncommon occurrence in the basin. It has been theorized that the deposition of ash in the basin helped fuel productivity in the water column and bottom water anoxia (Ettensohn, 1985a). In the study well, most of the ash is found in the lower Marcellus and corresponds to the highest levels of TOC. The only other ash found in the well was located in the middle Marcellus interval directly below the MFS and a peak in TOC (Fig. 18).

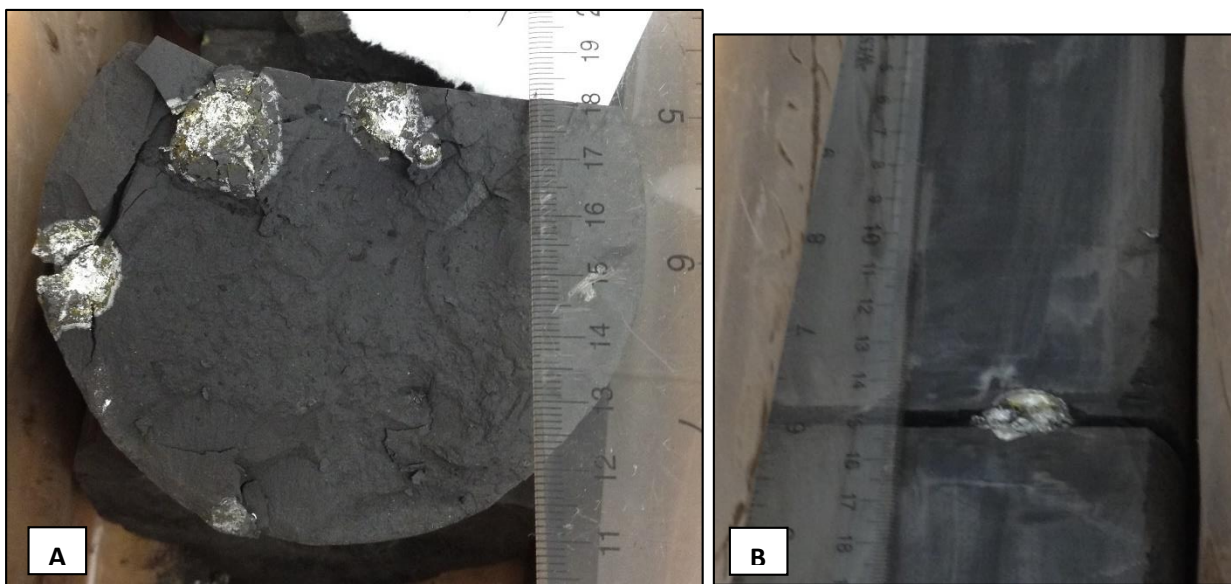


Figure 30. A) Image of ash pockets from top looking down on bedding plane. B) Side view of ash pocket with breakage along shale beds parallel to ash.

There were few natural fractures found in the lower Marcellus. The ones that were present were generally located on either side of the calcite concretions, and were calcite filled (Fig. 17). The shale was differentially compacted around the concretion, and had slickensides along the bedding planes. The shale on either side of the limestone layers at 7,206ft and 7,223ft have inclined bedding planes. The dip of the bedding gradually dies out and becomes horizontal as distance from the limestone layers increase.

Middle Marcellus:

The middle Marcellus was composed of 68% organic siliceous shale, 26% organic mixed shale, 4% gray mixed shale, and 2% carbonate intervals (Fig. 13). It had an average estimated TOC abundance of 14% by volume. The carbonate interval was at the base of the unit and the gray mixed shale was in the upper portion of the unit (Fig. 18). The two gray mixed shales were located directly beneath a calcite concretion and on top of a very calcite rich shale. While the facies composition of the middle Marcellus was very similar to the lower Marcellus there were eleven facies changes. The facies were more broken up and thinner than those in the lower Marcellus. There were four organic siliceous shale intervals mostly separated from one another by organic mixed shale of a 1.5 -3ft thick. The organic mixed shale intervals are estimated to be ductile. Due to their thicknesses and presence throughout the entire interval, fracture propagation would not be as easily achieved as in the lower Marcellus.

The middle Marcellus only had one centimeter scale pocket of ash. There was an increased abundance of visible pyrite. In the middle Marcellus there are intervals of medium gray shale present that were not seen in the lower Marcellus (Fig. 18). Based on the ECS facies and TOC estimation, the medium gray shale at 7,183ft was due to a lack of organic matter. The medium gray shale at 7,193ft was a result of an increased abundance of calcite. There were very few natural fractures present in the interval. There were some located around the calcite concretion at 7,182ft, and two at the very top of the middle Marcellus in the very calcitic shale that marked the end of the RST. The fractures were only a few centimeters to couple of inches long, generally calcite filled, and perpendicular to bedding.

Upper Marcellus:

The upper Marcellus was the most different out of the three Marcellus Formation intervals. There was a lot more of the gray shale intervals and organic mudstone present than found in the other two zones. There was only 39% organic siliceous shale and 9% organic mixed shale. There was 29% organic mudstone, 13% gray siliceous shale, 7% gray mixed shale, and 3% gray mudstone present in the interval (Fig. 13). The facies are all intermixed and do not have a repeated pattern. A possible explanation for the mixed facies of the upper Marcellus is an overall shallowing of the basin and closer proximity to land during deposition. A shallower basin would accommodate rapid changes in benthic conditions from non-oxygenated to oxygenated. There is a lot more gray shale facies in this interval than the other two. These gray shale facies are in direct contact with the black organic rich shale facies. The sharp contacts indicate a rapid change in bottom water conditions. There are nine such contacts in the upper Marcellus. These frequent changes would be more likely to occur in shallower water where stratification of the water column would more easily be destroyed.

In addition to the frequent, sharp facies changes from black organic rich shales to gray non-organic rich shales in the upper Marcellus, in the mineralogical logs there is a noticeable increase in the abundance of chlorite (Fig. 26). Chlorite is a clay mineral that typically forms from the alteration of terrestrially derived minerals. There are also burrows present at 7,158ft (Fig. 17). These burrows indicate that the bottom waters were oxygenated for periods of time. The burrows were later replaced with pyrite mineralization.

There were also, what appear to be debris from small turbidity currents at 7,171ft and 7,142ft (Fig. 17). In these deposits there is shell debris with random orientation, broken fragments, and gradually changed from very shelly at the base to shells floating in mud over approximately 2.5ft (Fig. 15). The debris was washed down from shallower water due to disturbances in the water column possibly caused by large storms. These were the only turbidity current deposits found in the formation, and both were located upper Marcellus interval. This further serves as indication that the environment of deposition at this time was in shallower water and closer to land than the Middle and lower Marcellus intervals.

While hard to see, the upper Marcellus had visible pyrite throughout the interval. The pyrite was typically present in the form of very small sparkles that could only be seen when the core surface was damp. There were some very thin, discontinuous, parallel to bedding fractures with pyrite mineralization from 7,150- 7,155ft and 7,160- 7,161ft (Fig. 17). From 7,152- 7,155 approximately 50% of the thin, discontinuous, parallel to bedding fracture were filled with calcite mineralization. The fractures from 7,150- 7,155ft were associated with a mixture organic mudstone, organic mixed shale, and gray siliceous shale facies. There were some larger natural fractures from 7,143- 7,148ft (Fig. 18). These fractures were a couple inches in length, had a lightning bolt shape, perpendicular to bedding, and calcite mineralization. The lithology in this interval was predominately organic siliceous shale.

Based on the estimated TOC log, the upper Marcellus has an average of 9.3% TOC by volume. This is the lowest of all three Marcellus Formation intervals. The lower amount of TOC, mixed lithologies and greater abundance of mudstone makes the upper Marcellus the poorest interval for production. In contrast, the high amount of TOC, lack of variation in facies, and limited facies changes makes the lower Marcellus the best target for production.

Regional Sequence Stratigraphy:

Two cross-sections that were chosen to represent the regional sequence stratigraphy were chosen to show how the formations change along strike (A-A') (Fig. 20) and down dip (B-B') (Fig. 21- 25). Along strike subsidence, and thus accommodation space, was greater to the northeast (Fig. 20). The Mahantango and Tully formations on lap on top of the Marcellus Formation, thin towards the southeast, and eventually pinch out. The Marcellus Formation also thins gradually towards the southeast, but pinches out further to the southeast than the Tully and Mahantango formations. Of the three Marcellus Formation intervals, the upper Marcellus thinned the most.

The down dip cross section (B- B') was flattened on each horizon from the L. Marcellus to the Tully formation to evaluate how subsidence changed over time, and to remove the effects of faulting that occurred during the deposition of the Mahantango and Tully formations (Fig. 21- 25). At the end of deposition of the lower Marcellus the greatest subsidence was towards the east at well #6 followed by wells #4 and #5 (Fig. 21). Subsidence continued to occur in wells #6- 8 at

an appreciable amount more than the wells to the west by the end of middle Marcellus deposition (Fig. 22).

When the down dip cross section was flattened on the U. Marcellus there was discernable increase in subsidence and accommodation space in wells #4 and #5 (Fig. 23). Well #4 is the Goff #55 study well. Wells #4- 8 continued to be more greatly affected by subsidence through time to the end of the Tully Formation (Fig. 24 & 25). Wells #2- 3 also begin to be more effected by subsidence after the deposition of the U. Marcellus. When flattened on the Mahantango Formation possible faulting could be seen between well #6 and well #7 (Fig. 24). Well #7 was displaced higher and this displacement becomes more pronounced in Figure 25 when flattened on the Tully Formation. Displacement could also be seen between well #4 and #5 in Figure 25.

The formations become thinner up dip to the west. As seen previously in the along strike cross section, the Mahantango and Tully formations on lap the Marcellus Formation. The Mahantango Formation pinched out between well #2 and #1 (Fig. 25). The Tully Formation was gradually thinning to a point of pinching out.

The study well was located in an area that received a moderate amount of accommodation space and along the slope leading down towards the deeper parts of the basin. The wells located further east would have been closer to the convergent boundary and would have underwent greater flexural subsidence. They would have also begun deepening first. The wells further east, closer to the orogeny, would have also receiver greater amounts of terrestrial clastic influx. This dilution could explain the repressed gamma-ray signature of well #8 in the B-B' cross-section.

CONCLUSIONS:

The Marcellus Formation was successfully divided into three intervals using a T-R sequence stratigraphic approach. These intervals were correlated across the region to other wells in the area. They were 3rd order T-R sequences that were largely controlled by sea level change. They were part of an overarching 2nd order T-R sequence that was most likely strongly controlled by flexural subsidence induced by lithospheric loading, with sea level change being of secondary importance.

The large scale T-R sequence extends from the base of the Marcellus to the Tully Formation. The lower Marcellus and TST of the middle Marcellus comprise the TST portion of the large scale T-R sequence. The RST of the middle Marcellus, upper Marcellus, Mahantango, and Tully formations make up the RST of the large T-R sequence. Pockets of ash are only found in the TST portion of the T-R sequence. The presence of ash indicates that there was active volcanism occurring along the eastern margin due to convergence. The absence of ash in the RST portion indicates that there was a stoppage in volcanic activity and decreased convergence. Therefore, flexural subsidence would have decreased a substantial amount. Decreased flexural subsidence would cause a TST deposition.

The black, organic rich shale of the Marcellus Formation was deposited in a reducing benthic environment. This was confirmed by the strong correlation between TOC and pyrite. However, the correlation was not strong enough for bottom water anoxia to be the sole reason for organic matter accumulation. Accumulation would have also been intimately related to overall productivity in the upper water column and clastic influx into the basin. Based on the relationship TOC had with the ash pockets, productivity in the water column may have been fueled partially by the ash. The direct relationship that pyrite had with the TST's and RST's of the Marcellus intervals indicate that fluctuations in sea level played a major role in the oxygen, or lack thereof, in the bottom waters. The relationship was strong enough such that a mineralogical log of pyrite abundance could be used to help aid in the separation of a black shale into T-R sequences.

The ECS facies developed using the advanced mineralogical logs provided an accurate representation of the formation. While the scale was larger than that of the core descriptions, it did generally account for the different lithologies. These facies were more quickly made than a core description, and could quantify the ratio of quartz to carbonate and TOC in a way that core descriptions cannot. The ECS lithofacies is an accurate representation of the well for the purposes of drilling, and the characterization of the reservoir can be trusted without the extra expenditure on core. However, the core is much more useful for finer scale details that can be used to decipher the history and depositional environment of the Marcellus Formation.

Of the ECS facies, the organic siliceous shale and organic mixed shale had the highest average TOC, respectively, and classified as brittle. These two facies are the primary targets in

the basin due to these characteristics. They were largely found, with the same relative abundance, in the lower and middle Marcellus intervals in the study well. The abundance of these facies in the lower half of the Marcellus was a main factor in the large amount of first year production of the study well.

The Goff #55, in Harrison County, WV was situated in an area that was dipping not only down dip but also along strike. The basin was dipping along strike due to the diminishing effects of flexural subsidence. In both cross sections the Tully and Mahantango formations pinch out against the Marcellus, and the upper Marcellus has thinned the most of the three Marcellus intervals. This type of on lapping and pinching out is to be expected due to the large T-R sequence. The lower Marcellus was deposited in a deeper more wide spread environment, while the later formations were deposited in shallower, gradually more restricted environments.

REFERENCES:

- Blakey, R., 2010, Middle Devonian (385Ma), North American Paleogeography. <http://www2.nau.edu/rcb7/globaltext2.html>, accessed October 13, 2014.
- Boggs, Sam, Jr. Principles of Sedimentology and Stratigraphy. 5th ed. Upper Saddle River, NJ: Pearson Prentice Hall, 2012. Print.
- Castle, J.W., 2001, Appalachian basin stratigraphic response to convergent-margin structural evolution: Basin Research, v. 13, p. 397-418.
- Catuneanu, O., and others, 2009, Towards the standardization of sequence stratigraphy. Earth Science Reviews 92, p. 1-33. <http://dx.doi.org/10.1016/j.earscirev.2008.10.003>
- Dennison, J., 1985, Catskill Delta shallow marine strata, in Woodrow, D.L., and Sevon, W.D., eds., The Catskill Delta: Geological Society of America special paper 201, p. 91-106.
- Ettensohn, F.R., 1985a, The Catskill Delta complex and the Acadian orogeny: A model, in Woodrow, D.L., and Sevon, W.D. (Eds.): The Catskill Delta: Geological Society America special paper 201, p. 39-49.
- Ettensohn, F.R., 1985b, Controls on development of Catskill Delta complex basin-facies, in Woodrow, D.L., and Sevon, W.D., (Eds.): The Catskill Delta: Geological Society of America Special Paper 201, p. 65-77.
- Ettensohn, F.R., 1992, Controls on the origin of the Devonian-Mississippian oil and gas shales, east-central United States: Fuel, v. 71, p. 1487-1492.
- Ettensohn, F.R., and Brett, C.E., 2002, Stratigraphic evidence from the Appalachian Basin for the continuation of the Taconian orogeny into Early Silurian time: Physics and Chemistry of the Earth, Parts A/B/C, v. 27, p. 279-288.
- Ettensohn, F.R., 2004, Modeling the nature and development of major Paleozoic clastic wedges in the Appalachian Basin, USA: Journal of Geodynamics, v. 37, p. 657-681.
- Fail, R.T., 1985, The Acadian orogeny and the Catskill Delta, in Woodrow, D. L., and Sevon, W.D., (Eds.): The Catskill Delta: Geological Society of America Special Paper 201, p. 15-37.
- Fail, R.T., 1997, A Geologic History of the Northern-Central Appalachians, Part 2: The Appalachian Basin from the Silurian through the Carboniferous: American Journal of Science, v. 297, p. 729-761.
- Glossary of Geology and Related Sciences, Amer. Geology. Inst., 1960, Washington D.C.

- Grieser, W., and Bray, J., 2007, Identification of production potential in unconventional reservoirs. SPE Paper: 106623.
- Jarvie, D. M., R. J. Hill, T. E. Ruble, and R. M. Pollastro, 2007, Unconventional shale-gas systems: The Mississippian Barnett Shale of North-Central Texas as one model for thermogenic shale-gas assessment: AAPG Bulletin, 91, 475–499, doi:10.1306/12190606068.
- Kent, D.V., 1985, Paleocontinental setting for the Catskill Delta, in Woodrow, D.L., and Sevon, W.D., (Eds.): The Catskill Delta: Geological Society of America Special Paper 201, p. 9-14.
- Lash, G.G., and Engelder T.J., 2011, Thickness trends and sequence stratigraphy of Middle Devonian Marcellus Formation, Appalachian Basin: Implications for Acadian foreland basin evolution. AAPG Bulletin, 95, 61–103.
- Lash, Gary G., and Blodd, David R., 2014, Organic matter accumulation, redox, and diagenetic history of the Marcellus Formation, southwestern Pennsylvania, Appalachian basin. Marine and Petroleum Geology 57, p. 244-263.
[http://dx.doi.org/10:1016/j.marpetgeo.2014.06.001](http://dx.doi.org/10.1016/j.marpetgeo.2014.06.001).
- Lazar, R.K., Bohacs, J.H., S. Macquaker, and J. Schieber, 2010, Fine-grained Rocks in Outcrops: Classification and Description Guidelines, in Schieber, J., Lazar, R., and Bohacs, K. eds., Sedimentology and stratigraphy of shale: American Association Petroleum Geologists 2010 Annual Convention in New Orleans Field Guide for Post-Convention Field Trip 10, p. 3-14.
- Mabesoone, Jannes M. and Neumann, Virginio H., 2005, Cyclic Development of Sedimentary Basins. (pp. 139-172). Elsevier. Online version available at:
<http://app.knovel.com/hotlink/toc/id:kpCDSB0001/cyclic-development-sedimentary/cyclic-development-sedimentary>.
- Murphy, J.B., and Keppie, J.D., 2005, The Acadian Orogeny in the Northern Appalachians, International Geology Review, 47:7, 663-687, DOI:10.2747/0020-6814.47.7.663
- Mullen, M. J., Roundtree, R., & Turk, G. A., 2007, A Composite Determination of Mechanical Rock Properties for Stimulation Design (What to Do When You Don't Have a Sonic Log): Society of Petroleum Engineers. doi:10.2118/108139-MS.
- NETL, 2010, Projecting the Economic Impact of Marcellus Shale Gas Development in West Virginia: A preliminary Analysis Using Publicly Available Data. Anthony M. Zammarilli.
- NETL, 2013, Modern Shale Gas Development in the United States: An Update.

- News and Information About Geology and Earth Science. Digital image. Geology.com: News and Information for Geology & Earth Science. Web. 15 Oct. 2014.
- Passey, Q.R., S. Creaney, J.B. Kulla, F.J. Moretti, and J.D. Stroud, 1990, A practical model for organic richness from porosity and resistivity logs. *AAPG Bulletin*, v. 74, p. 1777-1794.
- Rickman, R., Mullen, M., Petre, E., Grieser, B., and Kundert, D., 2008, A practical use of shale petrophysics for simulation design optimization: All shale plays are not clones of the Barnett Shale. SPE paper 115258.
- Schmoker, J. W., 1981, Determination of organic-matter content of Appalachian shales from gamma-ray logs. *AAPG Bulletin*, v. 65, p.1285-1298.
- Singh, P., 2008, Lithofacies and sequence stratigraphic framework of the Barnett Shale: Ph.D. dissertation, ConocoPhillips School of Geology and Geophysics: The University of Oklahoma.
- Slatt, R. M., Philp, P. R., Abousleiman, Y., Singh, P., Perez, R., Portas, R., Marfurt, K. J., Madrid-Arroyo, S., O'Brien, N., Eslinger, E. V., and Varuch, E. T., 2012, Pore-to-regional-scale Integrated Characterization Workflow for Unconventional Gas Shales, in J. A. Breyer, ed., *Shale Reservoirs- Giant Resources for the 21st Century: AAPG Memoir 97*, p. 127-150.
- Staal, C.R., Whalen, J.B., Vaquero, P.V., Zagorevski, A., and Rogers, N., 2009, Pre-Carboniferous, episodic accretion-related, orogenesis along the Laurentian margin of the northern Appalachians, in Murphy, J.B., Keppie., J.D., and Hynes, A.J., (Eds.): *Ancient Orogens and Modern Analogues: Geological Society, London, Special Paper 327*, p. 271-316. DOI: 10.1144/SP327.13
- Wang, Guochang. "Black Shale Lithofacies Prediction and Distribution Pattern Analysis of Middle Devonian Marcellus Shale in the Appalachian Basin, Northeastern U.S.A." Order No. 3530347 West Virginia University, 2012. Ann Arbor: ProQuest. Web. 22 Aug. 2015.
- Wang, F. P., and J. F. W. Gale, 2009, Screening criteria for shale-gas systems: *Gulf Coast Association of Geological Societies Transactions*, 59, 779–793.
- Wang, Guochang, and Carr, Timothy R., 2012, Methodology of organic-rich shale lithofacies identification and prediction: A case study from Marcellus Shale in the Appalachian basin: *Computers & Geosciences*, v. 49, p. 151-163.
- Wells, F., 2004, A New Method to Help Identify Unconventional Targets for Exploration and Development Through Integrative Analysis of Clastic Rock Property Fields: *Houston Geological Society Bulletin*, October issue, p. 35-49.
- WVGES O&G Record Reporting System. West Virginia Geological and Economic Survey, <http://www.wvgs.wvnet.edu/oginfo/pipeline/pipeline2.asp>, accessed Feb. 03, 2015.

Woodrow, D. L., 1985, Paleogeography, paleoclimate, and sedimentary processes of the Late Devonian Catskill Delta, in Woodrow, D.L., and Sevon, W.D., (Eds.): The Catskill Delta: Geological Society of America Special Paper 201, p. 51-63.

Zagorski, W. A., Wrightstone, G. R., Bowman, D. C., 2012, The Appalachian Basin Marcellus Gas Play: Its History of Development, Geologic Controls on Production, and Future Potential as a World-class Reservoir, in J.A. Breyer ed., Sale Reservoirs- Giant Resources for the 21st Century: AAPG Memoir 97, p. 172-200.

APPENDIX:

Core Description

Box Top 7123.0- Bottom & 7126.0: (Core 3, Box & Bag 7) (Figure A-1)

- **7,123.0 - 7,123.6:** Dark gray, flaggy, crinkly horizontal, V. pyritic, moderately to V. calcareous silty shale with abundant continuous and discontinuous horizontal relatively parallel to bedding fractures. Approximately 90% of fractures are calcite filled.
 - 7123.0 – 7123.3: It appears that once very calcitic layers (≤ 1 cm thick) are moderately replaced with pyrite. They now have a bronzy sheen and effervesce with HCL.
- **7123.6 – 7,124.9:** Dark gray to black, planar horizontal, pyritic, slightly calcareous, slightly fossiliferous silty shale with abundant horizontal, relatively parallel to bedding continuous and discontinuous fractures. Approximately 10% of fractures are calcite filled.
 - Pyrite → V. common. Has replaced some shells, formed mm scale nodules that are parallel to perpendicular to bedding, and also formed some thin (<1mm thick) laminations parallel to bedding.
 - 7124.1: Calcite nodule (4.5cm x 0.6cm) slightly replaced with pyrite. Has a bronzy sheen and effervesces with HCL.
- **7124.9 – 7126.0:** Black, flaggy, slightly crinkly/rugose horizontal, non-pyritic, non-calcareous silty shale with abundant continuous and discontinuous horizontal, relatively parallel to bedding fractures. Approximately 50% are calcite filled.
 - Throughout this section: V. abundant medium gray, non-calcareous, angular circled shaped crystals that are slightly raised from the surface. Average size is 1.5- 2mm. (Figure A-2).

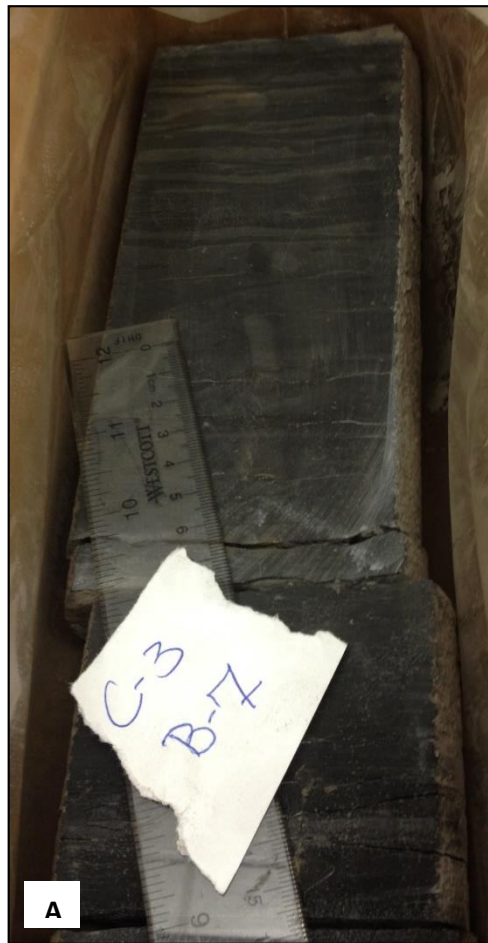


Figure A-1. A. top portion, B. middle portion, C. bottom portion of Core 3, Box & Bag 7



Figure A-2. An image of the abundant medium gray, non-calcareous, angular circled shaped crystals that are slightly raised from the surface.

Box Top 7126.0 – Bottom 7129.0: (Core 3, Box & Bag 8) (Figure A-3)

- **7126.0 - 7129.0:** Black, flaggy, bedding planes transitions from slightly crinkly at 7126.0 to planar at 7129.0, horizontal, non-calcareous, non-pyritic silty shale with abundant horizontal, relatively parallel to bedding, continuous and discontinuous fractures.
 - Throughout this section: abundant medium gray, non-calcareous, angular circled shaped crystals that are slightly raised from the surface. Average size is < 1mm.
 - **7128.75:** Mineralogy (Wt.%): 37% Silica, 60% Clay, 3% Carbonate.

Box Top 7129.0 – Bottom 7132.0: (Core 3, Box & Bag 9) (Figure A-4)

- **7129.0 – 7130.7:** Missing (7130.5: TOC= 4.46 Wt. %)
- **7130.7 – 7132.0:** From 7130.7 to 7131.0 black and from 7131.0 to 7132.0 dark gray, flaggy, planar horizontal bedding, non-calcareous, non- to slightly pyritic silty shale with abundant horizontal, relatively parallel to bedding, continuous and discontinuous fractures.
 - Throughout this section: abundant medium gray, non-calcareous, angular circled shaped crystals that are slightly raised from the surface. Average size is < 1mm. Also, these crystals are still common but not quite as abundant in the dark gray shale versus the black shale.

Box Top 7132.0 – Bottom 7133.8: (Core 3, Box & Bag 10) (Figure A-4)

- **7132.0 – 7133.8:** Dark gray to black, flaggy, planar horizontal bedding, non-calcareous, non-pyritic silty shale with abundant horizontal, parallel to bedding, continuous and discontinuous fractures.
 - Throughout this section: abundant medium gray, non-calcareous, angular circled shaped crystals that are slightly raised from the surface. Average size is much < 1mm.

****Note: no core/sample recovered for 7133.8 – 7134.0****



Figure A-3.
Picture of Core 3,
Box & Bag 8



Figure A-4.
Picture of Core 3,
Box & Bag 9

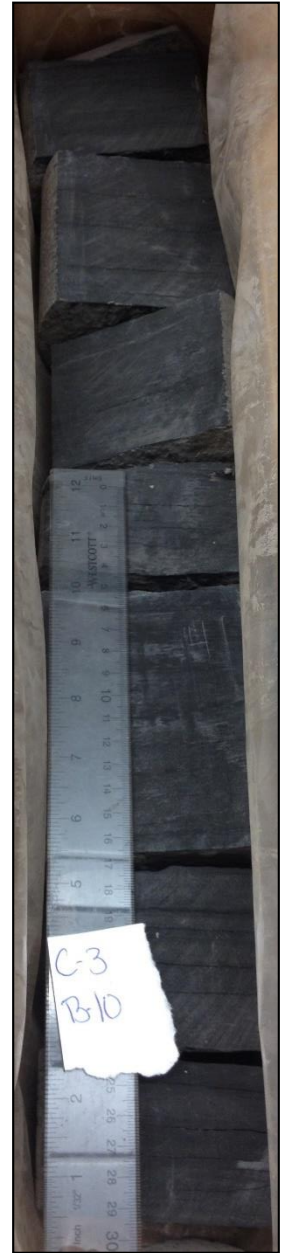


Figure A-5.
Picture of Core 3,
Box & Bag 10


Box Top 7134.0 – Bottom 7137.0: (Core 4, Box & Bag 1) (Figure A-6)

- **7134.0 – 7137.0:** Dark gray to black, flaggy, planar horizontal, non-calcareous, non- to V. slightly pyritic from 7134.0 to 7136.0 and slightly pyritic from 7136.0 to 7137.0 silty shale with abundant horizontal, relatively parallel to bedding, continuous and discontinuous fractures from 7134.0 to 7136.5.
 - **7135.3:** Mineralogy (Wt.%): 36% Silica, 63% Clay, 1% Carbonate.

Box Top 7137.0 – Bottom 7140.0: (Core 4, Box & Bag 2) (Figure A-7)

- **7137.0 – 7139.0:** Black, flaggy, planar horizontal, non-calcareous, non- to slightly pyritic silty shale with abundant horizontal, relatively parallel to bedding, continuous and discontinuous fractures.
 - V. slightly pyritic- can barely see bronze sparkles reflecting when moved in light and at 7138.45 there is a <1mm thick, continuous bronzy, pyrite lamination.
- **7139.0 – 7140.0:** Missing

Box Top 7140.0 – Bottom 7143.0: (Core 4, Box & Bag 3) (Figure A-8)

- **7140.0 – 7140.7:** Missing (7140.5: TOC= 2.55 Wt. %)
- **7140.7 – 7142.5:** Possible turbidity current.
 - **7140.7 – 7142.1:** Black, fossiliferous silty shale with planar horizontal bedding at 7140.7 that grades down to dark gray with crinkly/rugose bedding at 7142.1, flaggy, calcareous/ fossiliferous, non-pyritic wackestone.
 - Fossiliferous- abundance of seashells increases vertically with depth, and includes brachiopods () and fossil fragments.
 - **7141.25:** Mineralogy (Wt. %) 32% Silica, 49% Clay, 19% Carbonate.
 - **7142.1 – 7142.5:** Dark gray, flaggy, planar to slightly crinkly/rugose horizontal, decreasing vertically with depth from V. calcareous to slightly calcareous.
 - Calcareous- no visible shells/ skeletal fragments. From 7142.1 to 7142.25 there entire layers are wavy and medium gray due to laminations (wackestone), as the depth increases to from 7142.25 to 7142.5 the laminations gradually become short, discontinuous, V. thin (<0.5mm), medium gray laminations.

- **7142.5 – 7142.8:** V. dark gray to black, flaggy, planar horizontal, V. slightly calcareous, non-pyritic silty shale.
 - V. slightly calcareous- barely bubbles with HCL, and I can see little white specs.
- **7142.8 – 7143.0:** Black, flaggy, planar horizontal, non-calcareous, V. slightly pyritic silty shale.



Figure A-6.
Picture of Core 4,
Box & Bag 1



Figure A-7.
Picture of Core 4,
Box & Bag 2



Figure A-8.
Picture of Core 3,
Box & Bag 3

Box Top 7143.0 – Bottom 7146.0: (Core 4, Box & Bag 4) (Figure A-9)

- **7143.0 – 7144.5:** Dark gray to black, flaggy, planar horizontal, non-calcareous, non- to slightly pyritic silty shale with a sub-vertical, lightning bolt shaped, calcite filled fracture from 7144.3 to 7144.5.
- **7144.5 – 7146.0:** Dark gray to black, flaggy, planar horizontal, non-calcareous, non- to slightly pyritic silty shale with V. abundant sub-vertical, perpendicular to bedding fractures with a variety of orientations/strike and average thickness of 1mm.
 - This interval is extremely broken apart due to the fractures.

Box Top 7146.0 – Bottom 7149.0: (Core 4, Box & Bag 5) (Figure A-10)

- **7146.0 – 7146.25:** Dark gray to black, flaggy, planar horizontal, non- calcareous, non- to slightly pyritic silty shale with abundant horizontal, relatively parallel to bedding, continuous fractures.
- **7146.25 – 7146.9:** Dark gray, flaggy, planar horizontal, non-calcareous, non-pyritic silty shale with common horizontal, parallel to bedding, very thin (<0.5mm) continuous calcite filled fractures, and abundant sub-vertical, perpendicular to bedding calcite filled fractures with indiscernible orientation.
 - This whole interval is highly fractured and broken apart. Cannot tell what the original orientation of the sub-vertical fractures were or accurately place pieces back together.
- **7146.9 – 7148.0:** Dark gray to black, flaggy, planar horizontal, non- to slightly pyritic, non-calcareous silty shale with common horizontal, parallel to bedding, very thin (<0.5mm), continuous calcite filled fractures and common horizontal, parallel to bedding, ≤ 1.5 mm pyrite lamination from 7146.9 - 7147.0, and common sub-vertical to vertical, perpendicular to bedding, calcite filled fractures with a variety of orientations/strikes and an average thickness of 1mm from 7146.9 to 7148.0. Horizontal, relatively parallel to bedding, continuous fractures are abundant throughout the entire interval.
 - **7147.0 – 714.35:** Missing approximately 0.5inches of the left side of the core because of a perpendicular to viewing, vertical calcite filled fracture.
 - **7147.5 – 7148.0:** Core split in half parallel to viewing due to a parallel to viewing, vertical calcite filled fracture.
- **7148.0 – 7149.0:** Missing



A



B

Figure A-9. Picture of Core 4, Box & Bag 4.
A. Top portion. B. Bottom Portion.



Figure A-10. Picture of Core 4,
Box & Bag 5

Box Top 7149.0 – Bottom 7152.0: (Core 4, Box & Bag 6) (Figure A-11)

- **7149.0 – 7149.7:** Missing (7149.5: TOC= 4.28 Wt. %)
- **7149.7 – 7152.0:** Dark gray and black, flaggy, planar horizontal, non-calcareous, slightly pyritic silty shale.
 - Pyrite- Very short, very thin (<0.5mm), hard to see, parallel to bedding, discontinuous pyrite laminae throughout. Continuous, parallel to bedding, 1- 1.5mm thick pyrite laminations at 7150.5 and two at 7151.4.

Box Top 7152.0 – Bottom 7155.0: (Core 4, Box & Bag 7) (Figure A-12)

- **7152.0 – 7155.0:** Dark gray to black, flaggy, planar horizontal, non- to slightly calcareous, very slightly pyritic silty shale.
 - Pyrite & Calcite- Two millimeter scale nodules in the interval, and very faint/ hard to see discontinuous, parallel to bedding pyrite and calcite laminations.

Box Top 7155.0 – Bottom 7158.0: (Core 4, Box & Bag 8) (Figure A-13)

- **7155.0 – 7156.9:** Very dark gray to black, flaggy, planar horizontal, non-calcareous, non- to very slightly pyritic silty shale.
 - 7156.4- Pyrite nodule (1cm wide x 4.5mm thick).
 - 7156.85 – 7156.9: Dark gray, flaggy, crinkly/rugose horizontal, calcareous, non-pyritic silty shale.
- **7156.9 – 7157.5:** Missing
- **7157.5 – 7158.0:** Dark gray, flaggy, crinkly/rugose horizontal, very calcareous, moderately to very pyritic silty shale.
 - There appears to be a high abundance of burrows present that have been replaced with pyrite. Due to the abundance it is not possible to tell if they are fizzing in the presence of acid or if it is the shale. When dry the burrows have a medium gray coloration, however when damp they are very dark brown/bronze due to pyrite (Figure A-13B).



Figure A-11.
Picture of Core 4,
Box & Bag 6.

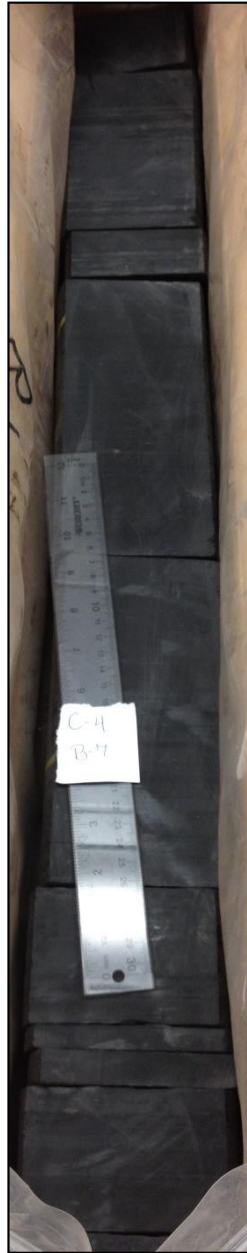


Figure A-12.
Picture of Core 4,
Box & Bag 7.



Figure A-13. Picture of Core 4, Box & Bag 8.
A. Top portion. **B.** Bottom Portion and possible burrows.

Box Top 7158.0 – Bottom 7161.0: (Core 4, Box & Bag 9) (Figure A-14)

- **7158.0 – 7159.7:** Missing (7159.0: TOC= 0.58 Wt. %)
- **7159.7 – 7161.0:** Dark gray to black, flaggy, planar, horizontal, non-calcareous, slightly to moderately pyritic silty shale with occasional very thin (<0.5mm) continuous and discontinuous calcite laminations.
 - Pyrite- short (<0.5cm long), very thin (<0.5mm) discontinuous pyrite laminations common throughout the interval and some millimeter scale pyrite nodules at the base of the unit.

Box Top 7161.0 – Bottom 7164.0: (Core 4, Box & Bag 10)

- (Missing Entire Box)
- **7162.45:** Mineralogy (Wt.%): 32% Silica, 57% Clay, 11% Carbonate.

Box Top 7164.0 – Bottom 7167.0: (Core 4, Box & Bag 11) (Figure A-15)

- **7164.0 – 7167.0:** Black, flaggy, planar horizontal, non- to slightly calcareous, slightly to moderately pyritic silty shale. Pyrite is present as very small, hard to see crystals throughout the interval, and five millimeter scale nodules from 7166.0 to 7166.6. At 7166.6 there is an almost perfect cubic (0.5cm x 0.5cm) pyrite crystal. At 7166.0 is a thin (approximate 0.5mm thick), continuous, parallel to bedding calcite lamination. At 7164.25 is a medium gray calcite concretion (3.8cm wide x 2.3cm thick). Shale is differentially compacted around the concretion and exhibits slickensides along bedding planes.

Box Top 7167.0 – Bottom 7170.0: (Core 4, Box & Bag 12) (Figure A-16)

- **7167.0 – 7167.5:** Black, flaggy, planar horizontal, slightly calcareous, non-pyritic silty shale with common faint, discontinuous, very thin (<0.5mm) calcite laminations.
- **7167.5 – 7168.2:** Black, flaggy, planar curved, slightly to moderately calcareous, non-pyritic silty shale differentially compacted around a medium gray, slightly pyritic around the edges, calcite concretion (8.5cm wide x 3.2cm thick) at 7167.85. The shale's calcite concentration increases closer to the concretion, and bedding planes near the calcite concretion exhibit slickensides. There are abundant medium gray, discontinuous, relatively parallel to bedding, calcite laminations 1 inch on either side of the calcite concretion. On 0.2 feet of either side of the concretion are calcite filled, thin (≤ 1 mm), dipping approximately 45° fractures.
 - The top and base of this interval correspond to the upper and lower limits of differential compaction.

- **7168.2 – 7168.7:** Black, flaggy, planar horizontal, non-calcareous, very pyritic silty shale. The pyrite is gold in coloration and form thin (<1mm), continuous and discontinuous, horizontal, parallel to bedding lamination that are on average separated by 2 to 5 millimeters.
- **7168.7 – 7168.95:** Black, flaggy, planar horizontal, non-calcareous, non-pyritic silty shale.
- **7168.95 – 7170.0:** Missing



Figure A-14.
Picture of Core 4,
Box & Bag 9.



Figure A-15.
Picture of Core 4,
Box & Bag 11.



Figure A-16.
Picture of Core 4,
Box & Bag 12.

Box Top 7170.0 – Bottom 7173.0: (Core 4, Box & Bag 13) (Figure A-17)

- **7170.0 – 7170.7:** Missing (7170.5: TOC= 4.71 Wt. %)
- **7170.7 – 7171.25:** This whole sequence is a turbidity current. Essentially grades from a wackestone at the base to a very calcareous silty shale at the top.
 - **7170.7 – 7170.9:** Dark gray, flaggy, slightly wavy sub-horizontal, slightly calcareous, non-pyritic, slightly fossiliferous silty shale.
 - **7170.9 – 7171.05:** Medium gray, flaggy, wavy sub-horizontal, moderately to very calcareous, non-pyritic, fossiliferous silty shale.
 - **7171.05 – 7171.25:** Light gray at base (0.5cm thick) and medium gray throughout the rest of the interval, flaggy, wavy/crinkly sub-horizontal, fossiliferous, very argillaceous limestone (wackestone). The unit becomes less argillaceous with depth and skeletal fragments become highly abundant.
- **7171.25 – 7171.45:** Black, flaggy, planar horizontal, non- to slightly calcareous, non-pyritic silty shale. Calcite is in the form of very thin (<0.5mm), discontinuous, parallel to bedding laminations.
- **7171.45 – 7172.05:** Black, flaggy, planar horizontal to sub-horizontal, non- to slightly calcareous, non-pyritic silty shale differentially compacted around 12 medium gray with a bronze sheen, non-calcareous, pyritic concretions that range in size from 0.5cm to 4cm in length and ≤12mm thick. Extending laterally from the sides of the concretion are 2mm or less thick lamination of pyrite. Due to the medium gray coloration of the concretions and bronze sheen, these were probably calcite concretions that were replaced with pyrite.
 - Along the exposed/separated bedding planes in this interval are brachiopod shells. These surfaces are slightly calcareous.
- **7172.05 – 7173.0:** Black, flaggy, planar horizontal, non-calcareous, slightly pyritic silty shale. Pyrite is in the form of small (<2mm), hard to see bronze and gold crystals throughout the interval.



Figure A-17. Picture of Core 4, Box & Bag 13 and features within that section. **A.** The upper portion of the core. **B.** The lower section of the core (continuing from where picture A stopped). **C.** A zoomed in image of the turbidity current. **D.** Image of seashells along bedding planes (location indicated by red arrow in image A).

Box Top 7173.0 – Bottom 7176.0: (Core 4, Box & Bag 14) (Figure A-18)

- **7173.0 – 7175.9:** Black, flaggy, planar horizontal, non-calcareous, non- to slightly pyritic silty shale.
- **7175.9 – 7176.0:** Dark gray to black, flaggy, planar horizontal, slightly calcareous, non-pyritic silty shale

Box Top 7176.0 – Bottom 7179.0: (Core 4, Box & Bag 15) (Figure A-19)

- **7176.0 – 7176.6:** Black, flaggy, planar horizontal, non-calcareous, slightly pyritic silty shale with a sub-vertical, thin (<1mm), bronze, pyrite filled fracture from 7176.5 to 7176.6.
- **7176.6 – 7178.1:** Medium gray, flaggy to slabby, crinkly/rugose horizontal, very calcareous, non-pyritic silty shale to very argillaceous wackestone -with light gray, 3- 4mm thick, parallel to bedding, calcite laminations at the top and base of the unit. From 7176.6 to 7177.5 is a thin (<1mm), sub-vertical, calcite filled fracture.
- **7178.1 – 7179.0:** Black, flaggy, planar sub-horizontal (dipping 8-10° to the right), non-calcareous, moderately pyritic silty shale. The pyrite in this interval forms continuous, parallel to bedding, bronze laminations that are 0.5cm thick at 7178.2 and 1.2cm thick at 7178.45.

Box Top 7179.0 – Bottom 7182.0: (Core 4, Box & Bag 16) (Figure A-20)

- **7179.0 – 7180.7:** Missing (7180.0: TOC= 3.98 Wt. %)
- **7180.7 – 7182.0:** Black with dark gray in middle (0.3ft), flaggy, planar sub-horizontal (dipping ~8° to the right at top of the unit and increasing a ~15° dip at the base), non-calcareous, non- to very slightly pyritic silty shale with a 1mm thick, subvertical, calcite filled fracture from 7181.8 to 7182.0.



Figure A-18.
Picture of Core 4,
Box & Bag 14.



Figure A-19.
Picture of Core 4,
Box & Bag 15.



Figure A-20.
Picture of Core 4,
Box & Bag 16.

Box Top 7182.0 – Bottom 7185.0: (Core 4, Box & Bag 17) (Figure A-21)

- **7182.0 – 7182.6:** Medium gray, slightly pyritic, argillaceous, calcite concretion with a black, non-calcareous, non-pyritic silty shale differentially compacted around the concretion. Along the outer edge of the concretion, within the shale, is a >1mm thick, very pyritic, calcite filled fracture dipping at ~60°.
- **7182.6 – 7183.0:** Black, flaggy, planar sub-horizontal (dipping ~15° to the left), non-calcareous, non-pyritic silty shale that has been cross cut by the very pyritic, calcite filled fracture from above. There are slickensides present along the bedding planes at 7182.6.
 - This unit was extremely broken apart and was pieced together as best as possible. The left inch or so of the core is missing or in smaller pieces spread throughout the box.
- **7183.0 – 7185.0:** Black with a dark gray interval from 7183.35 to 7183.7, flaggy, planar sub-horizontal (dipping ~15° - 20° to the left), non-calcareous, very slightly pyritic silty shale. Pyrite is in the form several (5) millimeter scale nodules.

Box Top 7185.0 – Bottom 7188.0: (Core 4, Box & Bag 18) (Figure A-22)

- **7185.0 – 7186.4:** Black, flaggy, planar sub-horizontal (dipping ~10° to the left), non-calcareous, non- to slightly pyritic silty shale. Pyrite is in the form of very thin to thin (<0.5mm - <1mm), continuous and discontinuous, parallel to bedding laminations, and is most common from 7185.75 to 7185.95. Elsewhere in the interval, there is little to no pyrite present.
- **7186.4 – 7188:** Black with three 0.15ft thick dark gray layers from 7187.25 to 7188.0, flaggy, planar horizontal, non-calcareous, non- to very slightly pyritic silty shale differentially compacted (0.1ft) around a medium gray with a slightly bronzy sheen, pyritic, argillaceous, calcite concretion at 7187.2 that is 4in wide and 1.5inches thick. Pyrite is slightly present throughout the concretion (causing the bronzy sheen), and forms a thin lamination along the inside of the concretion. Pyrite is present in the silty shale as very thin (<0.5mm), hard to see, discontinuous laminations.



Figure A-21. Picture of Core 4, Box & Bag 17. **A.** The upper portion of the core. **B.** The lower portion of core (continuing from where picture A stopped).



Figure A-22. Picture of Core 4, Box & Bag 18. **A.** The upper portion of the core. **B.** The lower portion of core (continuing from where picture A stopped).

Box Top 7188.0 – Bottom 7191.0: (Core 4, Box & Bag 19) (Figure A-23)

- **7188.0 – 7190.0:** Very dark gray and black, flaggy, planar horizontal, non-calcareous, non- to very slightly pyritic silty shale. Pyrite is present in this interval in the form of a few (6) millimeter to centimeter scale nodules. The size is 1cm wide by 2mm thick.
- **7190.0- 7191.0:** Missing

Box Top 7191.0 - Bottom 7193.9: (Core 4, Box & Bag 20) (Figure A-24)

- **7191.0 – 7191.7:** Missing (7191.5: TOC= 1.7 Wt. %)
- **7191.7 – 7193.3:** Black, flaggy, planar horizontal, non-calcareous, non- to very slightly pyritic silty shale. The pyrite in this interval is in the form of four millimeter scale nodules, and one faint laminae.
- **7193.3 – 7193.9:** Dark gray to black, flaggy, planar horizontal, slightly to moderately calcareous, non-pyritic silty shale.

Box Top 7194.0 – Bottom 7197.0: (Core 5, Box & Bag 1) (Figure A-25)

- **7194.0 – 7197.0:** Black, flaggy, planar horizontal and curved (at 7195.0 to 7195.2 and 7196.1), non-calcareous, non- to slightly pyritic silty shale with a light to medium gray with yellow staining, grainy/gritty, fibrous, circular (15mm x 15mm) ash pocket at 7196.0. Pyrite is present in the form of faint, hard to see, discontinuous, parallel to bedding laminations, millimeter scale nodules, and one 1cm thick, continuous, parallel to bedding lamination at 7195.7.



Figure A-23.
Picture of Core 4,
Box & Bag 19.



Figure A-24.
Picture of Core 4,
Box & Bag 20.



Figure A-25.
Picture of Core 5,
Box & Bag 1.

Box Top 7197.0 – Bottom 7200.0: (Core 5, Box & Bag 2) (Figure A-26)

- **7197.0 – 7198.8:** Black, flaggy, planar horizontal, non-calcareous, very slightly pyritic silty shale. Pyrite is in the form of very small, hard to see crystals throughout the interval.
- **7198.8 – 7199.7:** Missing
- **7199.7 – 7200.0:** Medium gray, non-pyritic, argillaceous calcite concretion. To the left of the core this medium gray unit has a curved vertically/circular edge and the rock is a dark gray, non-calcareous, non-pyritic silty shale. There is a very thin (<0.5mm), dipping ~60° to the right, calcite filled fracture from 7199.7-7199.9. There are two sub-horizontal, non-parallel to bedding, continuous fractures.

Box Top 7200.0 – Bottom 7203.0: (Core 5, Box & Bag 3) (Figure A-27)

- **7200.0 – 7200.7:** Missing (7200.0: TOC= 2.21 Wt. %)
- **7200.7 – 7202.0:** Black, flaggy, planar horizontal, non-calcareous, moderately pyritic silty shale. Very thin (<0.5mm), continuous and discontinuous, parallel to bedding, pyrite lamination with less than 2mm spacing can be seen when interval is damp.
 - **7201.1:** Mineralogy (Wt.%): 42% Silica, 56% Clay, 2% Carbonate.
- **7202.0 – 7202.7:** Missing (7202.5: TOC= 6.85 Wt. %)
- **7202.7 – 7203.0:** Black, flaggy, planar horizontal, non-calcareous, moderately pyritic silty shale. Thin (<1mm), continuous and discontinuous, parallel to bedding, pyrite laminations with less than 2mm in spacing present throughout interval.

Box Top 7203.0- Bottom 7206.0: (Core 5, Box & Bag 4) (Figure A-28)

- **7203.0 – 7203.5:** Black, flaggy, planar sun-horizontal (dipping to the right ~15°), non-calcareous, slightly to moderately pyritic silty shale. Pyrite is in the form of very thin (<0.5mm), hard to see unless damp, continuous and discontinuous, parallel to bedding laminations with an average vertical separation of 2- 4mm, and one pyrite nodule (15mm wide x 2mm thick).
- **7203.5 – 7204.0:** Black, flaggy, planar sub-horizontal (dipping to the right ~15°), very slightly calcareous, non-pyritic silty shale.
- **7204.0 – 7204.5:** Black, flaggy, planar sub-horizontal (dipping to the right ~15°), non- to very slightly calcareous, slightly to moderately pyritic silty shale. Pyrite is in the form of

three millimeter scale nodules, and very faint, hard to see unless damp, very thin (<0.5mm), continuous and discontinuous, parallel to bedding laminations from 7204.25 to 7205.0.

- **7204.5 – 7205.5:** Medium gray, flaggy, planar to rugose horizontal, very calcareous, non-pyritic wackestone (large calcite concretion?) with no skeletal debris and visible calcite crystals (<1mm in size).
- **7205.5 – 7206.0:** Missing



Figure A-26. Picture of Core 5, Box & Bag 2. **A.** The upper portion of core to the missing section. **B.** The lower portion of the core after the missing section

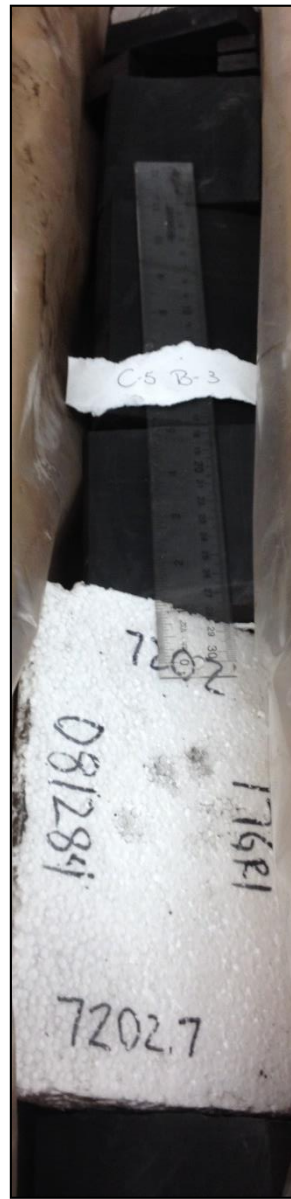


Figure A-27. Picture of Core 5, Box & Bag 3.



Figure A-28. Picture of Core 5, Box & Bag 4.

Box Top 7206.0 - Bottom 7209.0: (Core 5, Box & Bag 5) (Figure A-29)

- **7206.0 – 7207.0:** Medium gray, flaggy, rugose horizontal, very calcareous, non-pyritic except from 7206.85-7207.0 very pyritic, wackestone (large calcite concretion?) with no skeletal debris and visible calcite crystals (<1mm in size). From 7206.85 to 7207.0 pyrite is in the form of thick (2mm and 6mm) continuous, parallel to bedding, laminations. At 7207.0 there is an abrupt contact with the underlying unit.
- **7207.0 – 7207.35:** Black, flaggy, planar horizontal, non-calcareous, slightly pyritic silty shale with a light to medium gray, with yellow staining, grainy/gritty, fibrous ash pocket at 7207.35 that is oval in shape (4cm wide x 3cm long x 1.3cm thick). The bedding immediately adjacent to the ash has slickensides. A much smaller ash pocket is present however it is still embedded in the shale. The pyrite in this interval is in the form of very thin (<0.5mm) hard to see, continuous and discontinuous, parallel to bedding, laminations.
- **7207.35 – 7207.7:** dark gray, flaggy, planar to crinkly horizontal, moderately calcareous, non-pyritic silty shale. This interval was broken into a lot of chunks.
- **7207.7 – 7209.0:** Black, flaggy, planar horizontal, non- to slightly calcareous, non- pyritic silty shale with light to medium gray, with yellow staining, grainy/gritty, fibrous ash at 7208.0. There are four ash pockets on this surface that average in size 18mm long by 16mm wide and <3mm thick. The calcite in this interval is present as very faint, very thin (<0.5mm), discontinuous and continuous, parallel to bedding laminations.

Box Top 7209.0 – Bottom 7212.0: (Core 5, Box & Bag 6) (Figure A-30)

- **7209.0 – 7209.8:** Black, flaggy, planar horizontal, non- to very slightly calcareous, slightly pyritic silty shale. Pyrite is present in the form of faint, very thin (<0.5mm), continuous and discontinuous, parallel to bedding, laminations.
- **7209.8 – 7210.8:** Missing
- **7210.8 – 7211.0:** Black, flaggy, planar horizontal, non- to slightly calcareous, slightly pyritic silty shale. Pyrite is present in the unit as millimeter scale nodules and one 3cm wide by 3mm thick nodule.
- **7211.0 – 7211.7:** Missing (7211.0: TOC= 5.91 Wt. %)
- **7211.7 – 7212.0:** Black, flaggy, planar horizontal, non-calcareous, non-pyritic silty shale with slickensides present at 7211.7.

Box Top 7212.0 – Bottom 7215.0: (Core 5, Box & Bag 7) (Figure A-31)

- **7212.0 – 7215.0:** Black, flaggy, planar horizontal, non-calcareous, very slightly pyritic silty shale with a medium gray, argillaceous, moderately pyritic, calcite concretion from 7214.0 to 7214.6. The shale within 0.2ft of the concretion is differentially compacted around the concretion, has slickensides along bedding planes, and is moderately calcareous. The pyrite is present as very small (<0.5mm), hard to see crystals from 7212.0 to 7213.9, and there are several (9) millimeter scale nodules from 7214.6 – 7215.0.

Box Top 7215.0 – Bottom 7218.0: (Core 5, Box & Bag 8) (Figure A-32)

- **7215.0 – 7218.0:** Black, flaggy to slabby, planar horizontal, non- to slightly calcareous (from 7217.0 to 7218.0), non-pyritic silty shale with light to medium gray, with yellow staining, gritty/grainy, fibrous ash at 7216.1 and 7215.85 and have an average size of 5mm wide X 5mm long X 2mm thick. There are very small (<0.5mm) pyrite crystals next to the ash. At 7217.2 there are two sub-vertical (dipping ~40°), calcite filled fractures <1mm thick and 5-6cm long.
 - **7217.4:** Mineralogy (Wt.%): 44% Silica, 33% Clay, 23% Carbonate.

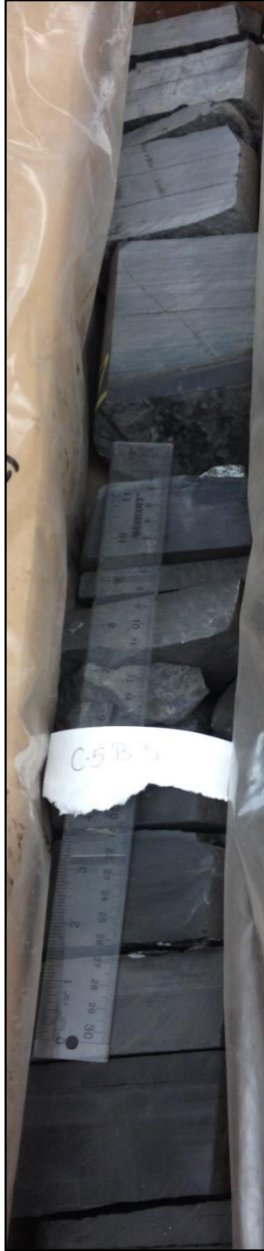


Figure A-29.
Picture of Core 5,
Box & Bag 5.



Figure A-30.
Picture of Core 5,
Box & Bag 6.



Figure A-31.
Picture of Core 5,
Box & Bag 7.



Figure A-32.
Picture of Core 5,
Box & Bag 8.

Box Top 7218.0 – Bottom 7221.0: (Core 5, Box & Bag 9) (Figure A-33)

- **7218.0 – 7220.0:** Black, flaggy, planar horizontal, non-calcareous, non- to slightly pyritic silty shale with light to medium gray, with yellow staining, grainy/gritty, fibrous ash at 7219.25. Pyrite is present as millimeter scale nodules throughout the interval, and thin (<1mm), continuous and discontinuous, parallel to bedding laminations.
- **7220.0 – 7221.0:** Missing

Box Top 7221.0 – Bottom 7224.0: (Core 5, Box & Bag 10) (Figure A-34)

- **7221.0 – 7221.7:** Missing (7221.0: TOC= 8.03 Wt. %)
- **7221.7 – 7222.6:** Dark gray, flaggy, planar sub-horizontal (dipping to the right ~10°), non-calcareous grading to moderately calcareous with depth, very slight pyritic silty shale.
- **7222.6 – 7224.0:** Medium gray, flaggy, very crinkly/rugose horizontal, wackestone (calcite concretion?).

Box Top 7224.0 – 7227.0: (Core 5, Box & Bag 11) (Figure A-35)

- **7224.0 – 7225.0:** Black, planar sub-horizontal (dipping to the left ~10° to ~15°), non-calcareous to slightly calcareous, non-pyritic silty shale with slickensides along bedding planes throughout the interval, and a lightning bolt shaped, vertical, calcite filled fracture that is 1mm thick x 7cm long, and spanning 4mm at 7224.8.
- **7225.0 – 7227.0:** Black, flaggy, planar sub-horizontal (dipping to the left ~8° to ~10°), non-calcareous, non- pyritic silty shale with slickensides along bedding planes throughout the interval, and two lightning bolt shaped, vertical, calcite filled fractures at 7225.2 (2mm thick x 3.5cm long, spanning 4cm) and at 7225.75 (1mm thick x 1.5cm long, spanning 5mm). There is light to medium gray, with yellow staining, grainy/gritty, fibrous ash at 7226.25 (cannot get measurements because within beds) and at 7226.8 (2cm wide x 2.5cm long x3.5cm thick).



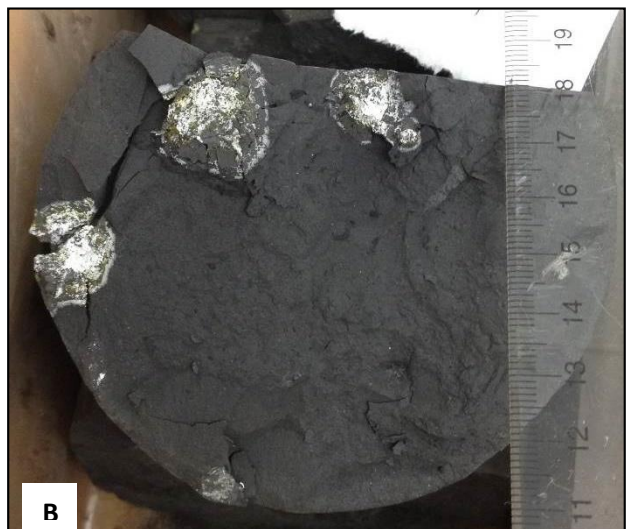
Figure A-33.
Picture of Core 5,
Box & Bag 9.



Figure A-34.
Picture of Core 5,
Box & Bag 10.



Figure A-35. Picture of
Core 5, Box & Bag 11.
A. Image of the entire
core from 7224.0 –
7227.0'. **B.** Image of
ash pockets (location
indicated by red arrow
in image A).



Box Top 7227.0 – 7230.0: (Core 5, Box & Bag 12) (Figure A-36)

- **7227.0 – 7227.45:** Dark gray, flaggy, planar horizontal, non-calcareous, slightly pyritic silty shale with slickensides along bedding parting at very top of the interval, and a sub-vertical, 1mm thick x 1.5cm long, calcite filled fracture.
- **7227.45 – 7227.7:** Missing
- **7227.7 – 7228.6:** From 7227.7 to 7227.9 is a dark gray, flaggy, planar horizontal, slightly calcareous, non-pyritic silty shale. From 7227.9 to 7228.2 is a medium to dark gray, flaggy, planar horizontal, very calcareous, non-pyritic wackestone. The calcite is present as a very high abundance of continuous, medium to thin (<2mm), continuous, parallel to bedding laminations. The lamination compose 70- 80% of this interval. 7228.2 to 7228.6 is a dark gray, flaggy, planar horizontal, moderately calcareous, non-pyritic silty shale. The calcite is present as thin (<1mm), continuous and discontinuous, parallel to bedding, laminations, and compose ~30- 40% of this interval. At 7228.35 are two, medium gray, sub-horizontal burrows. The contacts between these three units/intervals are abrupt/sharp.
- **7228.6 – 7228.8:** Medium gray, very calcareous, non-pyritic, argillaceous wackestone with no visible skeletal debris and sharp contacts above and below the interval.
- **7228.8 – 7228.9:** Dark gray to black, flaggy, planar sub-horizontal (dipping ~10- 15° to the right), moderately calcareous, non-pyritic silty shale. Calcite is present in the form of medium gray, thin (<1mm), discontinuous, parallel to bedding laminations.
- **7228.9 – 7229.9:** Missing
- **7229.9 – 7230.0:** Interbedded limestone and silty shale with ~70% being limestone. Limestone is medium gray and interbedded with discontinuous dark gray, wavy, beds of silty shale. There are skeletal fragments (≤1mm in length) throughout.

Box Top 7230.0 – Bottom 7233.0: (Core 5, Box & Bag 13) (Figure A-37)

- This box is alternating silty shale and argillaceous limestone beds.
- **7230.0 – 7230.7:** Missing (7230.5: TOC= 4.37 Wt. %)
- **7230.7 – 7231.24:** Interbedding of dark gray silty shale with medium gray, laminated to flaggy, crinkly horizontal, argillaceous wackestone.
- **7231.24 – 7231.53:** Missing

- **7231.53 – 7232.5:** Interbedding of silty shale and argillaceous wackestone with flaggy, horizontal bedding.
- **7232.5 – 7233.0:** Medium gray, flaggy, crinkly horizontal, fossiliferous, argillaceous wackestone. There are an abundance of crinoid fossils present. There is some interbedding of dark gray, thick (>2mm) laminations of silty shale.

Box Top 7233.0 – 7235.75: (Core 5, Box & Bag 14) (Figure A-38)

- Onondaga Limestone
- Medium gray, flaggy, crinkly/rugose horizontal, very fossiliferous, argillaceous wackestone. The fossils consist of crinoids, bryozoan, brachiopods, and corals. The 7233.0 to 7233.4 section is missing.



Figure A-36.
Picture of Core 5,
Box & Bag 12.



Figure A-37.
Picture of Core 5,
Box & Bag 13.



Figure A-38.
Picture of Core 5,
Box & Bag 14.

